Eur. Phys. J. B (2013) 86: 411
DOI: 10.1140/epjb/e2013-40333-7

THE EUROPEAN PHYSICAL JOURNAL B

Regular Article

Application of hierarchical equations of motion (HEOM) to time dependent quantum transport at zero and finite temperatures

Heng Tian[1] and GuanHua Chen[1,2,3,a]

[1] Department of Chemistry, The University of Hong Kong, Hong Kong, P.R. China
[2] Department of Physics, The University of Hong Kong, Hong Kong, P.R. China
[3] Centre for Theoretical and Computational Physics, The University of Hong Kong, Hong Kong, P.R. China

Received 10 April 2013 / Received in final form 9 July 2013
Published online 2 October 2013 – © EDP Sciences, Società Italiana di Fisica, Springer-Verlag 2013

Abstract. Going beyond the limitations of our earlier works [X. Zheng, F. Wang, C.Y. Yam, Y. Mo, G.H. Chen, Phys. Rev. B **75**, 195127 (2007); X. Zheng, G.H. Chen, Y. Mo, S.K. Koo, H. Tian, C.Y. Yam, Y.J. Yan, J. Chem. Phys. **133**, 114101 (2010)], we propose, in this manuscript, a new alternative approach to simulate time-dependent quantum transport phenomenon from first-principles. This new practical approach, still retaining the formal exactness of HEOM framework, does not rely on any intractable parametrization scheme and the pole structure of Fermi distribution function, thus, can seamlessly incorporated into first-principles simulation and treat transient response of an open electronic systems to an external bias voltage at both zero and finite temperatures on the equal footing. The salient feature of this approach is surveyed, and its time complexity is analysed. As a proof-of-principle of this approach, simulation of the transient current of one dimensional tight-binding chain, driven by some direct external voltages, is demonstrated.

1 Introduction

In the emergent field of molecular electronics, the steady-state current through ballistic molecular junctions, can be calculated from the Landauer-Büttiker formula reformulated in terms of non-equilibrium Green's functions (NEGF), coupled with the density functional theory (DFT) [1–3]. Though under much criticism, this approach is full-fledged and has been a routine part in several packages.

Nowadays to quantitatively characterize time-dependent quantum transport and reveal its fundamental process is on the cutting edge of research efforts, which is totally beyond the reach of the previous approach.

An appreciable number of related publications are available in recent decade. Zheng et al. [4] have proved the existence of a bijection between electron density function $\boldsymbol{\rho}_{\mathrm{D}}(\boldsymbol{r},t)$ of any finite region of a finite system and the external potential $v(\boldsymbol{r},t)$ which is real analytic with respect to both arguments. Consequently, they have proved the unique determination of Hamiltonian and all electronic properties of the whole dynamic system by this $\boldsymbol{\rho}_{\mathrm{D}}(\boldsymbol{r},t)$. They have named this result Holographic Time-Dependent Electron Density Theorem as the foundation of time-dependent density functional theory for open electronic system in parallel with the famous Runge-Gross theorem [5] for isolated electronic system. Formally exact though it is, unfortunately, this theorem did not show us the way to construct any explicit map between dissipation functional [6] and $\boldsymbol{\rho}_{\mathrm{D}}(\boldsymbol{r},t)$ directly. Rather, the following central equations in reference [4] are essentially the embodiment of NEGF,

$$i\dot{\boldsymbol{\sigma}}_{\mathrm{D}} = \left[\boldsymbol{h}_{\mathrm{D}}\left[t;\boldsymbol{\rho}_{\mathrm{D}}(\boldsymbol{r},t)\right],\boldsymbol{\sigma}_{\mathrm{D}}\right] - i\sum_{\alpha}\mathbf{Q}_{\alpha}\left[t;\boldsymbol{\rho}_{\mathrm{D}}(\boldsymbol{r},t)\right], \tag{1}$$

$$\mathbf{Q}_{\alpha}(t) = -\int_{-\infty}^{t} d\tau[\mathbf{G}^{r}(t,\tau)\boldsymbol{\Sigma}_{\alpha}^{<}(\tau,t) + \mathbf{G}^{<}(t,\tau)\boldsymbol{\Sigma}_{\alpha}^{a}(\tau,t)] + \mathrm{H.C.}, \tag{2}$$

$$\boldsymbol{\Sigma}_{\alpha}^{a}(\tau,t) = i\vartheta(t-\tau)\int_{-\infty}^{\infty} d\omega\boldsymbol{\Lambda}_{\alpha}(\omega)\, e^{i\omega(t-\tau)}e^{i\int_{\tau}^{t}\Delta_{\alpha}(\bar{t})d\bar{t}}, \tag{3}$$

$$\boldsymbol{\Sigma}_{\alpha}^{<}(\tau,t) = i\int_{-\infty}^{\infty} d\omega\; f_{\alpha}(\omega-\mu_{\alpha})\boldsymbol{\Lambda}_{\alpha}(\omega)\, e^{i\omega(t-\tau)}e^{i\int_{\tau}^{t}\Delta_{\alpha}(\bar{t})d\bar{t}}, \tag{4}$$

where $\boldsymbol{\sigma}_{\mathrm{D}}$ is the reduced single-particle density matrix (RSDM) for the device part, $\mathbf{G}^{</r}(t,\tau)$ is the two-time Green's function, $\boldsymbol{\Sigma}_{\alpha}^{<}(\tau,t)$ is the two-time lesser self-energy of the electrode α, $\boldsymbol{\Sigma}_{\alpha}^{a}(\tau,t)$ is the two-time advanced self-energy of the electrode α, $\vartheta(t-\tau)$ is the Heaviside step function, $\boldsymbol{\Lambda}_{\alpha}(\omega)$ is the line-width matrix of the electrode α, $f_{\alpha}(\omega-\mu_{\alpha})$ is the Fermi distribution function of the electrode α with the Fermi level μ_{α}

[a] e-mail: Ghc@everest.hku.hk

and $\Delta_\alpha(t)$ is the bias voltage applied on the electrode α. From here on, the subscript D in all related quantites will be omitted, if no confusion is invoked. This dissipation functional $\mathbf{Q}_\alpha(t)$ [6] in equation (2) at *zero* temperature has been crudely approximated by the so-called *Adiabatic* Wide-Band-Limit (AWBL) scheme in reference [4]. This treatment of the convolution integral in equation (2), i.e. the adiabatic approximation, has recently been transcended in the first author's thesis [7].

In order to make the integrations in equations (3) and (4) computed in an elementary way, the following scheme has been proposed in references [6,8,9]:

– multi-Lorentzian fitting

$$\boldsymbol{\Lambda}_\alpha(\omega) \approx \sum_{l=1}^{N_l} \frac{\eta_{\alpha l}}{(\omega - \Omega_{\alpha l})^2 + W_{\alpha l}^2} \bar{\boldsymbol{\Lambda}}_{\alpha l}, \tag{5}$$

with $\Omega_{\alpha l}$ being real, $W_{\alpha l} > 0$, and $\bar{\boldsymbol{\Lambda}}_{\alpha l}$ being a constant real symmetric matrix;

– Padé approximation of Fermi distribution function [10,11]

$$\frac{1}{1+e^x} - \frac{1}{2} \approx -\sum_{p=1}^{N_p} \left[\frac{r_p}{x - iz_p} + \frac{r_p}{x + iz_p} \right], \tag{6}$$

with $r_p > 0$, $z_p > 0$ and $N_p \in \mathbb{N}$.

If the Fermi level μ_α and the inverse temperature $\beta_\alpha = 1/(k_b T_\alpha)$ is considered, the above expansion should be adapted into

$$\begin{aligned} f_\alpha(\omega - \mu_\alpha) &= \frac{1}{1 + \exp\{\beta_\alpha(\omega - \mu_\alpha)\}} \\ &\approx \frac{1}{2} - \sum_{p=1}^{N_p} \left[\frac{R_p}{\omega - z_{\alpha p}} + \frac{R_p}{\omega - z_{\alpha p}^*} \right], \end{aligned} \tag{7}$$

where $z_{\alpha p} = \mu_\alpha + iz_p/\beta_\alpha$ and $R_p = r_p/\beta_\alpha$.

In consequence, $\boldsymbol{\Sigma}_\alpha^{</a}(\tau, t)$ is approximated by a sum of decaying exponentials. Then taking derivative with respect to t will result in a 2-tier HEOM [6,8,9], whose numerical solution can be obtained by various kinds of ordinary differential equation (ODE) solver.

However, the viability of multi-Lorentzian fitting for realistic systems where $\boldsymbol{\Lambda}_\alpha(\omega)$ is a matrix-valued function is doubtful. Besides, this kind of parametrization is likely to get the steady state current, if it exists, deviate from the result obtained from Landauer-Büttiker formula, which could be a great pitfall. More seriously, only at zero temperature does the first-principles simulation of a dynamic system have sound foundation [4,5] and physical meaning, in which case, unfortunately, this scheme may become numerically expensive. Therefore to design a first-principles-calculation-oriented framework is the main objective of this work.

This paper is outlined as follows. In Section 2, we give a self-contained elementary derivation of the 2-tier HEOM, which is equivalent to the one in references [6,8,9], but reformulated in a form convenient for manipulation later on in this work. Based on this new though equivalent form, in Section 3, a numerically feasible approach to solve this version of HEOM which still inherits the formal exactness is built step by step, followed by the initial condition of the 2-tier HEOM expounded in Section 4. As a preliminary application, in Section 5, simulation of dynamics of 1-dimensional homogeneous tight-binding chain is delivered, detailedly illustrating how this new approach is implemented. In Section 6, we place emphasis on the advantages of this new approach and some interesting simulation results; to conclude this work we point out some open issues for future exploration.

2 Elementary derivation of the HEOM for the noninterating system

Here we give a direct derivation of HEOM for a non-interacting system, without resorting to the advanced path-integral formalism for Fermion operators or the Keldysh contour. Throughout this work, the atomic unit is employed. Consider a non-interacting Kohn-Sham(KS) reference system of electrons with the Hamiltonian being:

$$\mathbf{H}_\mathrm{T} = \mathbf{H}_\mathrm{C} + \sum_\alpha \left(\mathbf{H}_\alpha + \mathbf{H}_{\alpha\mathrm{C}} \right), \tag{8}$$

where, $\mathbf{H}_\mathrm{C}$ denotes the KS Hamiltonian for the device part, $\mathbf{H}_\alpha$ the KS Hamiltonian for the electrode ($\alpha = \mathrm{L}, \mathrm{R}$), and $\mathbf{H}_{\alpha\mathrm{C}}$ the KS Hamiltonian for the tunneling between the device part and the electrode. In the language of second quantization they can be succinctly expressed as follows:

$$\mathbf{H}_\mathrm{C} = \sum_{\mu\nu} \boldsymbol{h}_{\mu\nu} a_\mu^\dagger a_\nu, \mathbf{H}_\alpha = \sum_{k\in\alpha} \epsilon_{\alpha k}\, d_{\alpha k}^\dagger d_{\alpha k}, \tag{9}$$

$$\mathbf{H}_{\alpha\mathrm{C}} = \sum_\mu \sum_{k\in\alpha} \boldsymbol{t}_{\alpha k\mu} d_{\alpha k}^\dagger a_\mu + \mathrm{H.C.}, \tag{10}$$

of which, $a_\mu^\dagger(a_\nu)$ creates (annihilates) an electron in the corresponding orthonormal basis $|\phi_\mu\rangle(|\phi_\nu\rangle)$ of the device part, and $d_{\alpha k}^\dagger(d_{\alpha k})$ creates (annihilates) an electron in the eigenstate $|k_\alpha\rangle$ of the electrode α. And accordingly, $\boldsymbol{h}_{\mu\nu} = \langle\mu|\hat{h}(\boldsymbol{r}, t)|\nu\rangle$, $\epsilon_{\alpha k} = \langle k_\alpha|\hat{h}(\boldsymbol{r}, t)|k_\alpha\rangle$, and $\boldsymbol{t}_{\alpha k\mu} = \langle k_\alpha|\hat{h}(\boldsymbol{r}, t)|\mu\rangle$.

It is more convenient to work in the reservoir $\mathbf{H}_\mathrm{B}$-interaction picture [8], where $\mathbf{H}_\mathrm{B} = \sum_\alpha \mathbf{H}_\alpha$. Note that $\{a_\mu^\dagger, d_{\alpha k}\} = 0 = \{a_\mu, d_{\alpha k}^\dagger\}$, hence, $\left[a_\mu^\dagger, \mathbf{H}_\mathrm{B}\right] = 0 = \left[a_\mu, \mathbf{H}_\mathrm{B}\right]$, which follows that $a_\mu^\dagger$'s and a_μ's stay the same under the transformation between the Schrödinger picture and the $\mathbf{H}_\mathrm{B}$-interaction picture. After transformation into this interaction picture, the Hamiltonian $\mathbf{H}_\mathrm{T}$ becomes

$$\tilde{\mathbf{H}}_\mathrm{T}(t) = \mathbf{H}_\mathrm{C} + \sum_\alpha \tilde{\mathbf{H}}_{\alpha\mathrm{C}}(t), \tag{11}$$

where

$$\tilde{\mathbf{H}}_{\alpha\mathrm{C}}(t)=\sum_{\mu}\left[\tilde{b}^{\dagger}_{\alpha\mu}(t)\,a_{\mu}+a^{\dagger}_{\mu}\tilde{b}_{\alpha\mu}(t)\right],$$
$$\tilde{b}^{\dagger}_{\alpha\mu}(t)=\sum_{k}\boldsymbol{t}_{\alpha k\mu}\tilde{d}^{\dagger}_{\alpha k}(t).$$

To facilitate later derivation, some stipulations are clarified from the beginning. As is known, any physical Hamiltonian should be bounded from below, so is $\mathbf{H}_{\alpha}$. Besides, $\mathbf{H}_{\alpha}$ is also bounded from above. Thereby, in this work, the whole discussion is restricted to the case where the spectra $\epsilon_{\alpha k}$'s are the same for different α and at least piece-wisely continuously distributed in a finite interval $[\omega_{min},\omega_{max}]$.

In the $\mathbf{H}_{\mathrm{B}}$-interaction picture,

$$\begin{aligned}\dot{\tilde{d}}^{\dagger}_{\alpha k}(t)&=-i\big[\tilde{d}^{\dagger}_{\alpha k}(t),\mathbf{H}_{\mathrm{B}}\big]\\&=i\left[\epsilon_{\alpha k}+\Delta_{\alpha}(t)\right]\tilde{d}^{\dagger}_{\alpha k}(t)\\\tilde{d}^{\dagger}_{\alpha k}(t)&=e^{i\int_{t_0}^{t}[\epsilon_{\alpha k}+\Delta_{\alpha}(\tau)]d\tau}\,\tilde{d}^{\dagger}_{\alpha k},\end{aligned}\tag{12}$$

in which $\Delta_{\alpha}(t)$ is the rigid uniform shift for all single-electron levels in electrode α under the time-dependent voltage on this electrode [12]. Thus,

$$\begin{aligned}\tilde{b}^{\dagger}_{\alpha\mu}(t)&=\sum_{k\in\alpha}\boldsymbol{t}_{\alpha k\mu}\tilde{d}^{\dagger}_{\alpha k}e^{i\int_{t_0}^{t}d\tau[\epsilon_{\alpha k}+\Delta_{\alpha}(\tau)]}\\&=\sum_{k\in\alpha}\int_{\omega_{min}}^{\omega_{max}}d\omega\,\delta(\omega-\epsilon_{\alpha k})\,e^{i\omega(t-t_0)}\\&\quad\times\boldsymbol{t}_{\alpha k\mu}\,\tilde{d}^{\dagger}_{\alpha k}\,e^{i\int_{t_0}^{t}d\tau\Delta_{\alpha}(\tau)}.\end{aligned}\tag{13}$$

Here, the same trick as the multiple-frequency-dispersed scheme in reference [8] is utilized. It is advantageous to work with the canonical interval $[-1,1]$. Here, having introduced two constants

$$\bar{\omega}=\frac{\omega_{max}+\omega_{min}}{2},\quad \Omega=\frac{\omega_{max}-\omega_{min}}{2},$$

the integrating interval $[\omega_{min},\omega_{max}]$ can be mapped into $[-1,1]$ via $x(\omega)=(\omega-\bar{\omega})/\Omega$, and accordingly,

$$\begin{aligned}\tilde{b}^{\dagger}_{\alpha\mu}(t)&=\Omega\sum_{k\in\alpha}\int_{-1}^{1}dx\,\delta(\Omega x+\bar{\omega}-\epsilon_{\alpha k})\\&\quad\times e^{i\Omega x(t-t_0)}\,\boldsymbol{t}_{\alpha k\mu}\,\tilde{d}^{\dagger}_{\alpha k}\,e^{i\int_{t_0}^{t}d\tau(\Delta_{\alpha}(\tau)+\bar{\omega})}.\end{aligned}\tag{14}$$

Let

$$\tilde{b}^{\dagger}_{\alpha\mu}(x,t)=\sum_{k\in\alpha}\delta\left(\Omega x+\bar{\omega}-\epsilon_{\alpha k}\right)\,\boldsymbol{t}_{\alpha k\mu}\,\tilde{d}^{\dagger}_{\alpha k}\,e^{i\int_{t_0}^{t}d\tau(\Delta_{\alpha}(\tau)+\bar{\omega})},\tag{15}$$

we have

$$\begin{aligned}\tilde{b}^{\dagger}_{\alpha\mu}(t)&=\Omega\int_{-1}^{1}dx\,e^{i\Omega x(t-t_0)}\tilde{b}^{\dagger}_{\alpha\mu}(x,t),\\\tilde{b}_{\alpha\mu}(t)&=\Omega\int_{-1}^{1}dx\,e^{-i\Omega x(t-t_0)}\tilde{b}_{\alpha\mu}(x,t),\end{aligned}\tag{16}$$

and

$$\begin{aligned}\tilde{\mathbf{H}}_{\alpha\mathrm{C}}(t)=\sum_{\mu}\Omega\int_{-1}^{1}dx\,&\Big[e^{i\Omega x(t-t_0)}\tilde{b}^{\dagger}_{\alpha\mu}(x,t)a_{\mu}\\&+a^{\dagger}_{\mu}e^{-i\Omega x(t-t_0)}\tilde{b}_{\alpha\mu}(x,t)\Big].\end{aligned}\tag{17}$$

Thereby the quantum Liouville equation reads

$$\begin{aligned}\dot{\tilde{\boldsymbol{\rho}}}_{\mathrm{T}}(t)&=-i\big[\tilde{\mathbf{H}}_{\mathrm{T}}(t),\tilde{\boldsymbol{\rho}}_{\mathrm{T}}(t)\big]=-i\mathcal{L}_{\mathrm{C}}\tilde{\boldsymbol{\rho}}_{\mathrm{T}}(t)\\&\quad-i\sum_{\alpha}\mathcal{L}_{\alpha\mathrm{C}}\tilde{\boldsymbol{\rho}}_{\mathrm{T}}(t),\end{aligned}\tag{18}$$

where the superoperators are defined as

$$\mathcal{L}_{\mathrm{C}}\cdot\equiv[\mathbf{H}_{\mathrm{C}},\cdot],\quad \mathcal{L}_{\alpha\mathrm{C}}\cdot\equiv\big[\tilde{\mathbf{H}}_{\alpha\mathrm{C}}(t),\cdot\big].\tag{19}$$

As the prime objective, the EOM for the RSDM,

$$\boldsymbol{\sigma}_{\mu\nu}(t)\equiv\mathrm{tr}_{\mathrm{T}}[a^{\dagger}_{\nu}a_{\mu}\rho_{\mathrm{T}}(t)]=\mathrm{tr}_{\mathrm{T}}[a^{\dagger}_{\nu}a_{\mu}\tilde{\boldsymbol{\rho}}_{\mathrm{T}}(t)],$$

is

$$\begin{aligned}i\dot{\boldsymbol{\sigma}}_{\mu\nu}(t)&=\mathrm{tr}_{\mathrm{T}}[a^{\dagger}_{\nu}a_{\mu}\,\mathcal{L}_{\mathrm{C}}\,\tilde{\boldsymbol{\rho}}_{\mathrm{T}}(t)]\\&\quad+\sum_{\alpha}\mathrm{tr}_{\mathrm{T}}[a^{\dagger}_{\nu}a_{\mu}\,\mathcal{L}_{\alpha\mathrm{C}}\,\tilde{\boldsymbol{\rho}}_{\mathrm{T}}(t)]\\&=\mathrm{tr}_{\mathrm{T}}\left\{\left[a^{\dagger}_{\nu}a_{\mu},\mathbf{H}_{\mathrm{C}}\right]\tilde{\boldsymbol{\rho}}_{\mathrm{T}}(t)\right\}\\&\quad+\sum_{\alpha}\mathrm{tr}_{\mathrm{T}}\left\{\left[a^{\dagger}_{\nu}a_{\mu},\tilde{\mathbf{H}}_{\alpha\mathrm{C}}(t)\right]\tilde{\boldsymbol{\rho}}_{\mathrm{T}}(t)\right\}\\&=[\boldsymbol{h}(t),\boldsymbol{\sigma}(t)]_{\mu\nu}-\sum_{\alpha}\left[\boldsymbol{\varphi}_{\alpha,\mu\nu}(t)-\boldsymbol{\varphi}^{\dagger}_{\alpha,\mu\nu}(t)\right]\\&=[\boldsymbol{h}(t),\boldsymbol{\sigma}(t)]_{\mu\nu}\\&\quad-\sum_{\alpha}\Omega\int_{-1}^{1}dx\sum_{\mu'}\mathrm{tr}_{\mathrm{T}}\Big\{\left[e^{i\Omega x(t-t_0)}\tilde{b}^{\dagger}_{\alpha\mu'}(x,t)a_{\mu}\,\delta_{\nu\mu'}\right.\\&\quad\left.-a^{\dagger}_{\mu}e^{-i\Omega x(t-t_0)}\tilde{b}_{\alpha\mu'}(x,t)\,\delta_{\mu\mu'}\right]\tilde{\boldsymbol{\rho}}_{\mathrm{T}}(t)\Big\}\\&=[\boldsymbol{h}(t),\boldsymbol{\sigma}(t)]_{\mu\nu}-\sum_{\alpha}\Omega\int_{-1}^{1}dx\,\Big[e^{i\Omega x(t-t_0)}\\&\quad\times\boldsymbol{\varphi}_{\alpha,\mu\nu}(x,t)-e^{-i\Omega x(t-t_0)}\boldsymbol{\varphi}^{\dagger}_{\alpha,\mu\nu}(x,t)\Big].\end{aligned}\tag{20}$$

Here, the second equality results from trace cycling invariance property; and the fourth follows the definition of first-tier auxiliary RSDM, $\boldsymbol{\varphi}_{\alpha,\mu\nu}(t)\equiv\mathrm{tr}_{\mathrm{T}}[\tilde{b}^{\dagger}_{\alpha\nu}(t)\,a_{\mu}\tilde{\boldsymbol{\rho}}_{\mathrm{T}}(t)]$, as well as its Hermitian conjugate $\boldsymbol{\varphi}^{\dagger}_{\alpha,\mu\nu}(t)=\mathrm{tr}_{\mathrm{T}}[a^{\dagger}_{\nu}\tilde{b}_{\alpha\mu}(t)\tilde{\boldsymbol{\rho}}_{\mathrm{T}}(t)]$; and the sixth follows the definition of the frequency-dispersed first-tier auxiliary RSDM

$$\begin{aligned}\boldsymbol{\varphi}_{\alpha,\mu\nu}(x,t)&\equiv\mathrm{tr}_{\mathrm{T}}\left[\tilde{b}^{\dagger}_{\alpha\nu}(x,t)\,a_{\mu}\,\tilde{\boldsymbol{\rho}}_{\mathrm{T}}(t)\right],\\\boldsymbol{\varphi}^{\dagger}_{\alpha,\mu\nu}(x,t)&\equiv\mathrm{tr}_{\mathrm{T}}\left[a^{\dagger}_{\nu}\,\tilde{b}_{\alpha\mu}(x,t)\,\tilde{\boldsymbol{\rho}}_{\mathrm{T}}(t)\right].\end{aligned}\tag{21}$$

Obviously, we have

$$\boldsymbol{\varphi}_{\alpha,\mu\nu}(t)=\Omega\int_{-1}^{1}dx\,e^{i\Omega x(t-t_0)}\boldsymbol{\varphi}_{\alpha,\mu\nu}(x,t)\tag{22}$$

$$\boldsymbol{\varphi}^{\dagger}_{\alpha,\mu\nu}(t)=\Omega\int_{-1}^{1}dx\,e^{-i\Omega x(t-t_0)}\boldsymbol{\varphi}^{\dagger}_{\alpha,\mu\nu}(x,t).\tag{23}$$

Next, we establish the EOM for the first-tier auxiliary RSDM, $\boldsymbol{\varphi}_{\alpha,\mu\nu}(x,t)$ just from its definition, as follows:

$$\begin{aligned}\dot{\boldsymbol{\varphi}}_{\alpha,\mu\nu}(x,t) &= \mathrm{tr}_{\mathrm{T}}\left\{\dot{\tilde{b}}^{\dagger}_{\alpha\nu}(x,t)\,a_{\mu}\,\tilde{\boldsymbol{\rho}}_{\mathrm{T}}(t)+\tilde{b}^{\dagger}_{\alpha\nu}(x,t)a_{\mu}\,\dot{\tilde{\boldsymbol{\rho}}}_{\mathrm{T}}(t)\right\}\\ &= i\left[\Delta_{\alpha}(t)+\bar{\omega}\right]\boldsymbol{\varphi}_{\alpha,\mu\nu}(x,t)\\ &\quad+\mathrm{tr}_{\mathrm{T}}\left\{\tilde{b}^{\dagger}_{\alpha\nu}(x,t)\,a_{\mu}\big[-i\mathcal{L}_{\mathrm{C}}\,\tilde{\boldsymbol{\rho}}_{\mathrm{T}}(t)\big]\right\}\\ &\quad+\sum_{\alpha'}\mathrm{tr}_{\mathrm{T}}\left\{\tilde{b}^{\dagger}_{\alpha\nu}(x,t)\,a_{\mu}\big[-i\mathcal{L}_{\alpha'\mathrm{C}}\,\tilde{\boldsymbol{\rho}}_{\mathrm{T}}(t)\big]\right\}\\ &= i\left[\Delta_{\alpha}(t)+\bar{\omega}\right]\boldsymbol{\varphi}_{\alpha,\mu\nu}(x,t)\\ &\quad-i\sum_{\mu'}\big[\boldsymbol{h}_{\mu\mu'}\,\boldsymbol{\varphi}_{\alpha,\mu'\nu}(x,t)\\ &\quad-\boldsymbol{\sigma}_{\mu\mu'}(t)\,\boldsymbol{\Lambda}_{\alpha,\mu'\nu}(x,t)\big]\\ &\quad-i\Omega\sum_{\alpha'}\int_{-1}^{1}dx'\,e^{-i\Omega x'(t-t_0)}\\ &\quad\times\mathrm{tr}_{\mathrm{T}}\left\{\tilde{b}^{\dagger}_{\alpha\nu}(x,t)\,\tilde{b}_{\alpha'\mu}(x',t)\,\tilde{\boldsymbol{\rho}}_{\mathrm{T}}(t)\right\}. \qquad (24)\end{aligned}$$

Here,

$$\boldsymbol{\Lambda}_{\alpha,\mu\nu}(x,t)\equiv\sum_{k\in\alpha}\delta(\Omega x+\bar{\omega}-\epsilon_{\alpha k})\boldsymbol{t}^{*}_{\alpha k\mu}\boldsymbol{t}_{\alpha k\nu}e^{-i\Omega x(t-t_0)}$$

is introduced, and when $t=t_0$ it reduces to the so-called line-width matrix $\boldsymbol{\Lambda}_{\alpha,\mu\nu}(x)=-\Im\boldsymbol{\Sigma}^{r}_{\alpha,\mu\nu}(x)/\pi$, where the retarded self-energy $\boldsymbol{\Sigma}^{r}_{\alpha}(x)$ results from the open system boundary conditions of the device in the presence of the semi-infinite electrode α.

It is apt to mistake the last term for

$$\begin{aligned}&-i\Omega\sum_{\alpha'}\sum_{k\in\alpha}\sum_{k'\in\alpha'}\int_{-1}^{1}dx'\delta(\Omega x+\bar{\omega}-\epsilon_{\alpha k})\\ &\quad\times\delta(\Omega x'+\bar{\omega}-\epsilon_{\alpha' k'})e^{-i\Omega x(t-t_0)}\boldsymbol{t}_{\alpha k\nu}\,\boldsymbol{t}^{*}_{\alpha' k'\mu}\delta_{\alpha\alpha'}\delta_{kk'}\\ &\qquad\times\left[if_{\alpha}\left(\epsilon_{\alpha k}\right)\right]=-i\boldsymbol{\Lambda}_{\alpha,\mu\nu}(x,t)\,\bar{f}_{\alpha}(x), \qquad (25)\end{aligned}$$

where $f_{\alpha}(\epsilon)=1/[\exp\{\beta_{\alpha}(\epsilon-\mu_{\alpha})\}+1]$ is the Fermi distribution function for the electrode α at temperature $T_{\alpha}=1/(k_b\beta_{\alpha})$ along with μ_{α} being the equilibrium Fermi energy for the electrode α; $\bar{f}_{\alpha}(x)=f_{\alpha}(\Omega x+\bar{\omega})$ is introduced to simplify the notation. In the partition-free scheme [13] employed here, the whole system without any bias voltage should possess a unique equilibrium Fermi energy μ_0 and a unique temperature T, as required by the grand canonical ensemble, thus $\bar{f}_{\alpha}(x)$ is the same for different α. In fact, equation (25) corresponds to an extreme situation where there is no tunneling between the device and the electrode, with the density matrix being denoted as $\tilde{\boldsymbol{\rho}}_{\mathrm{T}}(-\infty)$. That is to say,

$$\begin{aligned}&-i\Omega\sum_{\alpha'}\int_{-1}^{1}dx'\,e^{-i\Omega x'(t-t_0)}\\ &\qquad\times\mathrm{tr}_{\mathrm{T}}\left\{\tilde{b}^{\dagger}_{\alpha\nu}(x,t)\,\tilde{b}_{\alpha'\mu}(x',t)\,\tilde{\rho}_{\mathrm{T}}(-\infty)\right\}=\\ &\qquad\qquad-i\boldsymbol{\Lambda}_{\alpha,\mu\nu}(x,t)\,\bar{f}_{\alpha}(x).\end{aligned}$$

After separating this part out of the original one, the remnant can be defined as the second-tier auxiliary RSDM,

$$\begin{aligned}\boldsymbol{\psi}_{\alpha'\alpha,\mu\nu}(x',x,t)&=\mathrm{tr}_{\mathrm{T}}\left\{\tilde{b}^{\dagger}_{\alpha\nu}(x,t)\,\tilde{b}_{\alpha'\mu}(x',t)\right.\\ &\qquad\left.\times\left[\tilde{\boldsymbol{\rho}}_{\mathrm{T}}(t)-\tilde{\boldsymbol{\rho}}_{\mathrm{T}}(-\infty)\right]\right\}. \qquad (26)\end{aligned}$$

The final form of EOM equation (24) for the first-tier auxiliary RSDM, $\boldsymbol{\varphi}_{\alpha,\mu\nu}(\omega,t)$, turns out to be

$$\begin{aligned}i\dot{\boldsymbol{\varphi}}_{\alpha,\mu\nu}(x,t)&=-\left[\Delta_{\alpha}(t)+\bar{\omega}\right]\boldsymbol{\varphi}_{\alpha,\mu\nu}(x,t)\\ &\quad+\sum_{\mu'}\boldsymbol{h}_{\mu\mu'}\boldsymbol{\varphi}_{\alpha,\mu'\nu}(x,t)\\ &\quad-\sum_{\mu'}\boldsymbol{\sigma}_{\mu\mu'}(t)\boldsymbol{\Lambda}_{\alpha,\mu'\nu}(x,t)\\ &\quad+\bar{f}_{\alpha}(x)\boldsymbol{\Lambda}_{\alpha,\mu\nu}(x,t)\\ &\quad+\Omega\sum_{\alpha'}\int_{-1}^{1}dx'\,e^{-i\Omega x'(t-t_0)}\boldsymbol{\psi}_{\alpha'\alpha,\mu\nu}(x',x,t). \qquad (27)\end{aligned}$$

Based on equation (26), it is relatively easy to obtain the EOM for the second-tier auxiliary RSDM, $\boldsymbol{\psi}_{\alpha'\alpha,\mu\nu}(x',x,t)$, as follows:

$$\begin{aligned}\dot{\boldsymbol{\psi}}_{\alpha'\alpha,\mu\nu}(x',x,t)&=i\left[\Delta_{\alpha}(t)+\bar{\omega}\right]\boldsymbol{\psi}_{\alpha'\alpha,\mu\nu}(x',x,t)\\ &\quad-i\left[\Delta_{\alpha'}(t)+\bar{\omega}\right]\boldsymbol{\varphi}_{\alpha'\alpha,\mu\nu}(x',x,t)\\ &\quad+\mathrm{tr}_{\mathrm{T}}\left[\tilde{b}^{\dagger}_{\alpha\nu}(x,t)\,\tilde{b}_{\alpha'\mu}(x',t)\,\dot{\tilde{\boldsymbol{\rho}}}_{\mathrm{T}}(t)\right]\\ &=i\left[\Delta_{\alpha}(t)-\Delta_{\alpha'}(t)\right]\boldsymbol{\psi}_{\alpha'\alpha,\mu\nu}(x',x,t)\\ &\quad-i\sum_{\mu'}\boldsymbol{\Lambda}^{*}_{\alpha',\mu\mu'}(x',t)\boldsymbol{\varphi}_{\alpha,\mu'\nu}(x,t)\\ &\quad+i\sum_{\mu'}\boldsymbol{\varphi}^{\dagger}_{\alpha',\mu\mu'}(x',t)\boldsymbol{\Lambda}_{\alpha,\mu'\nu}(x,t). \qquad (28)\end{aligned}$$

Now, the HEOM equations (20), (27) and (28) have been established as the exact framework in this work.

3 New practical approach

In fact, it is the dissipation functional $\mathbf{Q}_{\alpha}(t)$ [6]

$$\begin{aligned}\mathbf{Q}_{\alpha}(t)&=-i\left[\boldsymbol{\varphi}_{\alpha}(t)-\boldsymbol{\varphi}^{\dagger}_{\alpha}(t)\right]\\ &=-i\Omega\left[\int_{-1}^{1}dx\,e^{-i\Omega x\left(t-t_0\right)}\boldsymbol{\varphi}_{\alpha}\left(x,t\right)\right.\\ &\quad\left.-e^{i\Omega x\left(t-t_0\right)}\boldsymbol{\varphi}^{\dagger}_{\alpha}\left(x,t\right)\right], \qquad (29)\end{aligned}$$

which affects the dynamics of RSDM, and the transient current

$$I_{\alpha}\left(t\right)=-\mathrm{tr}_{\mathrm{T}}\left[\mathbf{Q}_{\alpha}(t)\right], \qquad (30)$$

that are of primary concern, but not $\boldsymbol{\varphi}_\alpha(x,t)$ or $\boldsymbol{\psi}_{\alpha'\alpha}(x',x,t)$ themselves. This is the main guideline for the development of the new practical method to solve the HEOM. As is seen in equation (29), in order to obtain $\mathbf{Q}_\alpha(t)$, the finite range Fourier transform with respect to x must be performed. However, it is unwise to blindly apply the commonly used Gaussian quadrature to the integration of an oscillatory function [14]. Moreover, since the analytic expression of the function $\boldsymbol{\varphi}_\alpha(x,t)$ is unavailable, we cannot devise a quadrature rule grounded on the characteristic of this function.

Actually, the high precision quadrature rules of the Fourier integral of the same kind as equation (29) can be traced back to Bakhvalov and Vasileva [15] and Patterson [16]. The technique of the latter has its origin in the famous Jacobi-Anger identity,

$$e^{itx} = J_0(t) + \sum_{n=1}^{\infty} 2i^n J_n(t)\, T_n(x) \quad \forall t \in \mathbb{R}, \forall x \in [-1,1]. \tag{31}$$

Here, $J_n(t)$ is the Bessel function of the first kind of integer order, and $T_n(x)$ is the Chebyshev polynomial of the first kind [17]. This identity in effect decomposes the Fourier kernel e^{-ixt} into Chebyshev polynomials with respect to the argument $x \in [-1,1]$ in the spirit of the method of separation of variables. In the context of our problem, the following decomposition

$$e^{-i\Omega x(t-t_0)} = J_0(\Omega(t-t_0)) + \sum_{n=1}^{\infty} 2(-i)^n J_n(\Omega(t-t_0))\, T_n(x) \tag{32}$$

makes the integral in equation (29) ready to calculate, provided that the following modified moment

$$\boldsymbol{\varphi}_{\alpha,k}(t) = (2-\delta_{k,0}) \int_{-1}^{1} dx T_k(x) \boldsymbol{\varphi}_\alpha(x,t), \quad k \in \mathbb{N}, \tag{33}$$

is known. Here, $\boldsymbol{\varphi}_{\alpha,k}(t)$ for any time $t > t_0$ can be considered as the solution of its EOM,

$$\begin{aligned}\frac{i}{2-\delta_{k,0}}\dot{\boldsymbol{\varphi}}_{\alpha,k}(t) &= i\int_{-1}^{1} dx\, T_k(x)\dot{\boldsymbol{\varphi}}_\alpha(x,t)\\ &= [\boldsymbol{h}(t) - \bar{\omega} - \Delta_\alpha(t)]\frac{\boldsymbol{\varphi}_{\alpha,k}(t)}{2-\delta_{k,0}}\\ &\quad + \Omega\sum_{k'=0}^{\infty}\frac{(-i)^{k'}J_{k'}(\Omega(t-t_0))}{2-\delta_{k,0}}\boldsymbol{\psi}_{\alpha'k',\alpha k}(t)\\ &\quad - \boldsymbol{\sigma}(t)\int_{-1}^{1} dx\, T_k(x)\boldsymbol{\Lambda}_\alpha(x,t)\\ &\quad + \int_{-1}^{1} dx\, T_k(x)\bar{f}_\alpha(x)\boldsymbol{\Lambda}_\alpha(x,t)\end{aligned} \tag{34}$$

in which the modified moment

$$\boldsymbol{\psi}_{\alpha'k',\alpha k}(t) = (2-\delta_{k',0})(2-\delta_{k,0})\int_{-1}^{1} dx'\, T_{k'}(x') \times \int_{-1}^{1} dx\, T_k(x)\boldsymbol{\psi}_{\alpha',\alpha}(x',x,t) \tag{35}$$

is introduced.

It is observed that the integral

$$\boldsymbol{\Pi}_{\alpha,k}(t) = \int_{-1}^{1} dx\, T_k(x)\boldsymbol{\Lambda}_\alpha(x,t)$$

in equation (34) can be calculated independently, also on the basis of equation (32),

$$\begin{aligned}\boldsymbol{\Pi}_{\alpha,k}(t) &= \int_{-1}^{1} dx\, T_k(x)\boldsymbol{\Lambda}_\alpha(x)e^{-i\Omega x(t-t_0)}\\ &= \frac{J_0(\Omega(t-t_0))\,\boldsymbol{\Lambda}_{\alpha,k}}{2-\delta_{k,0}}\\ &\quad + \sum_{n=1}^{\infty}\frac{(-i)^n J_n(\Omega(t-t_0))\,\boldsymbol{\Lambda}_{\alpha,k+n}}{2}\\ &\quad + \sum_{n=1}^{\infty}\frac{(-i)^n J_n(\Omega(t-t_0))\,\boldsymbol{\Lambda}_{\alpha,|k-n|}}{2-\delta_{k,n}}\end{aligned} \tag{36}$$

where

$$\boldsymbol{\Lambda}_{\alpha,k} = (2-\delta_{k,0})\int_{-1}^{1} dx T_k(x)\boldsymbol{\Lambda}_\alpha(x). \tag{37}$$

It seems that

$$\boldsymbol{\Xi}_{\alpha,k}(t) = \int_{-1}^{1} dx\, T_k(x)\bar{f}_\alpha(x)\boldsymbol{\Lambda}_\alpha(x,t)$$

in equation (34) cannot be more easily evaluated otherwise than by the same equation (32) based strategy,

$$\begin{aligned}\boldsymbol{\Xi}_{\alpha,k}(t) &= \int_{-1}^{1} dx\, T_k(x)\bar{f}_\alpha(x)\boldsymbol{\Lambda}_\alpha(x)e^{-i\Omega x(t-t_0)}\\ &= \sum_{n=1}^{\infty}(-i)^n J_n(\Omega(t-t_0))\\ &\quad \times \int_{-1}^{1} dx\, \bar{f}_\alpha(x)T_{k+n}(x)\,\boldsymbol{\Lambda}_\alpha(x)\\ &\quad + \sum_{n=1}^{\infty}(-i)^n J_n(\Omega(t-t_0))\\ &\quad \times \int_{-1}^{1} dx\, \bar{f}_\alpha(x)T_{|k-n|}(x)\,\boldsymbol{\Lambda}_\alpha(x)\\ &\quad + J_0(\Omega(t-t_0))\int_{-1}^{1} dx\, T_k(x)\bar{f}_\alpha(x)\boldsymbol{\Lambda}_\alpha(x).\end{aligned} \tag{38}$$

The time-independent part of equation (38) is expected to be provided beforehand.

Similar manipulation can be applied to equation (28), which is just a verbatim repetition of the procedure leading to equation (34). Heretofore, we have completed the discretization of HEOM equations (20), (27) and (28), which now reduce into the following set of coupled ODEs:

$$\begin{aligned} i\dot{\boldsymbol{\sigma}}(t) &= [\boldsymbol{h}(t), \boldsymbol{\sigma}(t)] - \sum_{\alpha}\sum_{k=0}^{\infty}\left[\Omega i^k J_k(\Omega(t-t_0))\right. \\ &\quad \left.\times \boldsymbol{\varphi}_{\alpha,k}(t) - \text{H.C.}\right], \qquad (39) \\ i\dot{\boldsymbol{\varphi}}_{\alpha,k}(t) &= [\boldsymbol{h}(t) - \bar{\omega} - \Delta_\alpha(t)]\,\boldsymbol{\varphi}_{\alpha,k}(t) \\ &\quad + (2-\delta_{k,0})\left[\boldsymbol{\Xi}_{\alpha,k}(t) - \boldsymbol{\sigma}(t)\,\boldsymbol{\Pi}_{\alpha,k}(t)\right] \\ &\quad + \sum_{\alpha'}\sum_{k'=0}^{\infty}(-i)^{k'}\,\Omega J_{k'}(\Omega(t-t_0))\boldsymbol{\psi}_{\alpha' k',\alpha k}(t), \qquad (40) \end{aligned}$$

$$\begin{aligned} i\dot{\boldsymbol{\psi}}_{\alpha' k',\alpha k}(t) &= (2-\delta_{k'0})\boldsymbol{\Pi}^*_{\alpha',k'}(t)\boldsymbol{\varphi}_{\alpha,k}(t) \\ &\quad - (2-\delta_{k0})\boldsymbol{\varphi}^\dagger_{\alpha',k'}(t)\boldsymbol{\Pi}_{\alpha,k}(t) \\ &\quad + [\Delta_{\alpha'}(t) - \Delta_\alpha(t)]\,\boldsymbol{\psi}_{\alpha' k',\alpha k}(t), \qquad (41) \end{aligned}$$

where $\boldsymbol{\Xi}_{\alpha,k}(t)$'s and $\boldsymbol{\Pi}_{\alpha,k}(t)$'s are obtained from equations (38) and (36), respectively.

Here, it is high time to stress the advantage of this new approach. From reference [18], we learn that

$$J_n(t) \sim \frac{1}{\sqrt{2\pi n}}\left(\frac{te}{2n}\right)^n \quad \text{as } n\to\infty, \quad \text{for a given } t, \qquad (42)$$

which indicates that $J_n(t)$ decays spectrally with respect to n. Therefore, the sum of the first M terms of the series in equations (39), (40), (36) and (38) already numerically converges, with M being around $1.5\Omega(t-t_0)$, provided $\Omega(t-t_0)$ is large enough. In the meantime the ensuing truncation error can be made negligible, compared with the numerical error of ODE solver, if criterion of trunction is appropriately chosen and the initial condition is exactly evaluated. Consequently, the error mainly comes from the practical numerical integrator of ODE, e.g. fourth-order Runge-Kutta algorithm.

Obviously, as the propagation time goes longer, more and more $\boldsymbol{\varphi}_{\alpha,k}(t)$'s contribute to the transient dynamics. More specifically, in numerical implementation, it is the desired span of maximum propagation time multiplied by the system-dependent constant Ω that determines the number of $\boldsymbol{\varphi}_{\alpha,k}(t)$'s as well as $\boldsymbol{\psi}_{\alpha' k',\alpha k}(t)$'s needed. Be cautious that although at early stage only the first few $\boldsymbol{\varphi}_{\alpha,k}(t)$'s are included in summation, it is indispensable to simultaneously update the whole set of unknown matrices involved from the very start till the end.

Moreover, in striking contrast to scheme proposed previously [6,9] with the purpose of approximating Fermi distribution function $\bar{f}_\alpha(x)$ on the whole real axis, in the present approach, whether the actural behavior of $\bar{f}_\alpha(x)$ outside the interval $[-1,1]$ can be reproduced is not of concern.

4 Initial condition

We have completed half of our journey towards the end, i.e. having formulated the law of transient dynamics of the device, the remaining half is to determine the initial state of the dynamics. Rather than do this job within a particular framework, equations (39), (40) and (41), without loss of generality, we prefer to examine the original HEOM equations (20), (27) and (28).

Physical intuition is that in absence of bias voltage as the driving force, the total system described by $\mathbf{H}_{\rm T}$ is in the equilibrium state, which means the RSDM $\boldsymbol{\sigma}$ should keep the same despite the lapse of time, i.e. the left-hand side (LHS) of equation (20) vanishes. But it is ungrounded to let the LHS of equations (27), (28) be zero. To proceed, it is best to change the interaction picture back to the Schrödinger picture.

In the grand canonical equilibrium state,

$$\boldsymbol{\rho}_{\rm T}(t_0) = e^{\beta(\mathbf{H}_{\rm T}-\mu_0\mathbf{N})}\Big/\mathrm{tr}_{\rm T}\, e^{\beta(\mathbf{H}_{\rm T}-\mu_0\mathbf{N})}, \qquad (43)$$

thus the solution of quantum Liouville equation is

$$\boldsymbol{\rho}_{\rm T}(t) = e^{i\mathbf{H}_{\rm T}(t-t_0)}\boldsymbol{\rho}_{\rm T}(t_0)e^{-i\mathbf{H}_{\rm T}(t-t_0)} = \boldsymbol{\rho}_{\rm T}(t_0). \qquad (44)$$

Using this identity, it is trivial to see that

$$\begin{aligned} \boldsymbol{\sigma}_{\mu\nu}(t) &\equiv \mathrm{tr}_{\rm T}[a^\dagger_\nu a_\mu \boldsymbol{\rho}_{\rm T}(t)] \\ &= \mathrm{tr}_{\rm T}[a^\dagger_\nu(t_0)a_\mu(t_0)\boldsymbol{\rho}_{\rm T}(t_0)] \\ &= \boldsymbol{\sigma}_{\mu\nu}(t_0). \qquad (45) \end{aligned}$$

However, equation (44) has some further implications as follows:

$$\begin{aligned} \boldsymbol{\varphi}_{\alpha,\mu\nu}(x,t) &\equiv \mathrm{tr}_{\rm T}\left\{\tilde{f}^\dagger_{\alpha\nu}(x,t)\,a_\mu\,\tilde{\rho}_{\rm T}(t)\right\} \\ &= e^{-i\Omega x(t-t_0)}\mathrm{tr}_{\rm T}\left\{e^{i\Omega x(t-t_0)}\tilde{b}^\dagger_{\alpha\nu}(x,t)\,a_\mu\,\tilde{\boldsymbol{\rho}}_{\rm T}(t)\right\} \\ &= e^{-i\Omega x(t-t_0)}\mathrm{tr}_{\rm T}\left\{\tilde{b}^\dagger_{\alpha\nu}(x,t_0)\,a_\mu\,\rho_{\rm T}(t_0)\right\} \\ &= e^{-i\Omega x(t-t_0)}\boldsymbol{\varphi}_{\alpha,\mu\nu}(x,t_0), \qquad (46) \end{aligned}$$

and similarly,

$$\boldsymbol{\psi}_{\alpha'\alpha,\mu\nu}(x',x,t) = e^{-i\Omega(x-x')(t-t_0)}\boldsymbol{\psi}_{\alpha'\alpha,\mu\nu}(x',x,t_0). \qquad (47)$$

To put it simply, $e^{i\Omega x(t-t_0)}\boldsymbol{\varphi}_{\alpha,\mu\nu}(x,t)$ and $e^{i\Omega(x-x')(t-t_0)}\boldsymbol{\psi}_{\alpha'\alpha,\mu\nu}(x',x,t)$ are time-invariant in the equilibrium state.

Now, it is quite clear that

$$i\dot{\boldsymbol{\varphi}}_{\alpha,\mu\nu}(x,t_0) = \Omega x\boldsymbol{\varphi}_{\alpha,\mu\nu}(x,t_0) \qquad (48)$$

$$i\dot{\boldsymbol{\psi}}_{\alpha'\alpha,\mu\nu}(x',x,t_0) = \Omega(x-x')\,\boldsymbol{\psi}_{\alpha'\alpha,\mu\nu}(x',x,t_0), \qquad (49)$$

which generally do not vanish.

These results, compared with the general HEOM equations (20), (27) and (28), lead to the following coupled equations,

$$[\boldsymbol{h}(t_0),\boldsymbol{\sigma}(t_0)] = \sum_{\alpha} \Omega \int_{-1}^{1} dx \left[\boldsymbol{\varphi}_{\alpha}(x,t_0) - \boldsymbol{\varphi}_{\alpha}^{\dagger}(x,t_0)\right] \tag{50}$$

$$\begin{aligned}\Omega x\boldsymbol{\varphi}_{\alpha}(x,t_0) = {} & [\boldsymbol{h}(t_0)-\bar{\omega}]\,\boldsymbol{\varphi}_{\alpha}(x,t_0) \\ & - \boldsymbol{\sigma}(t_0)\boldsymbol{\Lambda}_{\alpha}(x) + \bar{f}_{\alpha}(x)\boldsymbol{\Lambda}_{\alpha}(x) \\ & + \Omega\sum_{\alpha'}\int_{-1}^{1} dx'\,\boldsymbol{\psi}_{\alpha'\alpha}(x',x,t_0)\end{aligned} \tag{51}$$

$$\begin{aligned}\Omega\,(x-x')\,\boldsymbol{\psi}_{\alpha'\alpha}(x',x,t_0) = {} & \boldsymbol{\Lambda}_{\alpha'}(x')\boldsymbol{\varphi}_{\alpha}(x,t_0) \\ & - \boldsymbol{\varphi}_{\alpha'}^{\dagger}(x',t_0)\boldsymbol{\Lambda}_{\alpha}(x).\end{aligned} \tag{52}$$

These three equations are supposed to be accordingly discretized, so as to provide the initial condition for equations (39), (40) and (41).

Unfortunately, for any given $k_{max} \in \mathbb{N}$, there will always be some higher order modified moments $\boldsymbol{\varphi}_{\alpha,k_{max}+1}(t_0)$, $\boldsymbol{\psi}_{\alpha'k'_{max}+1,\alpha k}(t_0)$ and $\boldsymbol{\psi}_{\alpha'k',\alpha k_{max}+1}(t_0)$, involved with $k,k' \leq k_{max}$, if we directly follow the same procedure in Section 3. That is to say, it is unlikely that the initial condition can be found by solving a self-closed linear equations. To determine the initial condition is another major obstacle of the present approach.

To make the best use of the basic relations equations (33), (35) and (37) at $t = t_0$ is the only way out, so far as we know. Since at $t = t_0$ the system is in the equilibrium state, the Matsubara (imaginary time) Green's function [19] is the most suitable tool for our problem.

Comparing equation (21) with the Matsubara Green's function,

$$\begin{aligned}\mathbf{G}^{M}_{\mu\alpha k}(\tau,\tau') &= -\mathrm{tr}_{\mathrm{T}}\left[\mathbf{T}_{\tau}a_{\mu}(t_0-i\tau)\tilde{d}^{\dagger}_{\alpha k}(t_0-i\tau')\boldsymbol{\rho}_{\mathrm{T}}(t_0)\right] \\ &= \mathbf{G}^{M}_{\mu\alpha k}(0,\tau'-\tau),\end{aligned} \tag{53}$$

where $\mathbf{T}_{\tau}$ is the time-ordering operator in imaginary time, it is easy to identify

$$\begin{aligned}\boldsymbol{\varphi}_{\alpha,\mu\nu}(x,t_0) &\equiv \mathrm{tr}_{\mathrm{T}}\left[\tilde{b}^{\dagger}_{\alpha\nu}(x,t_0)\,a_{\mu}\,\boldsymbol{\rho}_{\mathrm{T}}(t_0)\right] \\ &= \sum_{k\in\alpha}\delta\left(\Omega x+\bar{\omega}-\epsilon_{\alpha k}\right)\,\mathrm{tr}_{\mathrm{T}} \\ &\quad\times\left[\tilde{d}^{\dagger}_{\alpha k}\,a_{\mu}\,\boldsymbol{\rho}_{\mathrm{T}}(t_0)\right]\boldsymbol{t}_{\alpha k\nu} \\ &= \lim_{\eta\to 0^{+}}\sum_{k\in\alpha}\delta\left(\Omega x+\bar{\omega}-\epsilon_{\alpha k}\right) \\ &\quad\times\mathbf{G}^{M}_{\mu\alpha k}(0,\eta)\,\boldsymbol{t}_{\alpha k\nu}.\end{aligned} \tag{54}$$

As is known to all, the Matsubara Green's function observes the Kubo-Martin-Schwinger boundary condition [20,21], i.e. the following identity holds,

$$\mathbf{G}^{M}(0,\eta) = -\mathbf{G}^{M}(0,\eta+\beta). \tag{55}$$

Thus, Matsubara Green's function is periodic with a periodicity of 2β. Due to this periodicity, Matsubara Green's function can be represented by its Fourier series,

$$\mathbf{G}^{M}_{\mu\alpha k}(0,\eta) = \frac{1}{\beta}\sum_{n\in\mathbb{Z}}\mathbf{G}^{M}_{\mu\alpha k}(i\omega_n)\,e^{-i\omega_n\eta}, \tag{56}$$

where $\omega_n = (2n+1)\,\pi/\beta$ is the so-called fermionic Matsubara frequecy. In frequency domain, the Matsubara Green's function can be defined analogously to the retarded Green's function. Solely with some basic linear algebra knowledge, we have

$$\begin{aligned}\mathbf{G}^{M}(i\omega_n) &= \begin{bmatrix}\mathbf{G}^{M}_{LL}(i\omega_n) & \mathbf{G}^{M}_{LC}(i\omega_n) & \mathbf{G}^{M}_{LR}(i\omega_n)\\ \mathbf{G}^{M}_{CL}(i\omega_n) & \mathbf{G}^{M}_{C}(i\omega_n) & \mathbf{G}^{M}_{CR}(i\omega_n)\\ \mathbf{G}^{M}_{RL}(i\omega_n) & \mathbf{G}^{M}_{RC}(i\omega_n) & \mathbf{G}^{M}_{RR}(i\omega_n)\end{bmatrix} \\ &= \left((i\omega_n+\mu_0)\,\boldsymbol{I} - \begin{bmatrix}\boldsymbol{h}_L & \boldsymbol{t}_{LC} & \mathbf{0}\\ \boldsymbol{t}_{CL} & \boldsymbol{h}_C & \boldsymbol{t}_{CR}\\ \mathbf{0} & \boldsymbol{t}_{RC} & \boldsymbol{h}_R\end{bmatrix}\right)^{-1},\end{aligned} \tag{57}$$

$$\begin{aligned}\mathbf{G}^{M}_{C}(i\omega_n) &= \left[(i\omega_n+\mu_0)\boldsymbol{I}_C - \boldsymbol{h}_C - \boldsymbol{\Sigma}_L(i\omega_n) - \boldsymbol{\Sigma}_R(i\omega_n)\right]^{-1} \\ &= \left[(i\omega_n+\mu_0)\boldsymbol{I}_C - \boldsymbol{h}_C - \boldsymbol{t}_{LC}\mathbf{g}_L(i\omega_n)\boldsymbol{t}_{CL} - \boldsymbol{t}_{RC}\mathbf{g}_R(i\omega_n)\boldsymbol{t}_{CR}\right]^{-1},\end{aligned} \tag{58}$$

$$\mathbf{g}^{M}_{L/R}(i\omega_n) = \left[(i\omega_n+\mu_0)\,\boldsymbol{I} - \boldsymbol{h}_{L/R}\right]^{-1}, \tag{59}$$

$$\mathbf{G}^{M}_{CL}(i\omega_n) = \mathbf{G}^{M}_{C}(i\omega_n)\,\boldsymbol{t}_{CL}\mathbf{g}^{M}_{L}(i\omega_n), \tag{60}$$

$$\mathbf{G}^{M}_{CR}(i\omega_n) = \mathbf{G}^{M}_{C}(i\omega_n)\,\boldsymbol{t}_{CR}\mathbf{g}^{M}_{R}(i\omega_n), \tag{61}$$

$$\begin{aligned}\mathbf{G}^{M}_{LL}(i\omega_n) = {} & \mathbf{g}^{M}_{L}(i\omega_n) + \mathbf{g}^{M}_{L}(i\omega_n)\,\boldsymbol{t}_{LC} \\ & \times\mathbf{G}^{M}_{C}(i\omega_n)\,\boldsymbol{t}_{CL}\mathbf{g}^{M}_{L}(i\omega_n),\end{aligned} \tag{62}$$

$$\begin{aligned}\mathbf{G}^{M}_{RR}(i\omega_n) = {} & \mathbf{g}^{M}_{R}(i\omega_n) + \boldsymbol{g}^{M}_{R}(i\omega_n)\,\boldsymbol{t}_{RC} \\ & \times\mathbf{G}^{M}_{C}(i\omega_n)\,\boldsymbol{t}_{CR}\mathbf{g}^{M}_{R}(i\omega_n),\end{aligned} \tag{63}$$

$$\mathbf{G}^{M}_{LR}(i\omega_n) = \mathbf{g}^{M}_{L}(i\omega_n)\,\boldsymbol{t}_{LC}\mathbf{G}^{M}_{C}(i\omega_n)\,\boldsymbol{t}_{CR}\mathbf{g}^{M}_{R}(i\omega_n). \tag{64}$$

Owing to these results, we have

$$\begin{aligned}\boldsymbol{\varphi}_{\alpha\mu\nu}(x,t_0) &= \lim_{\eta\to 0^+}\frac{1}{\beta}\sum_n\sum_{k\in\alpha}\delta(\Omega x+\bar{\omega}-\epsilon_{\alpha k})\\ &\quad\times G^M_{\mu\alpha k}(i\omega_n)\,\boldsymbol{t}_{\alpha k\nu}e^{-i\omega_n\eta}\\ &= \lim_{\eta\to 0^+}\frac{1}{\beta}\sum_{n\in\mathbb{Z}}\sum_{\nu'}\sum_{k\in\alpha}\delta(\Omega x+\bar{\omega}-\epsilon_{\alpha k})\\ &\quad\times G^M_{\mu\nu'}(i\omega_n)\,\boldsymbol{t}^*_{\alpha k\nu'}\frac{1}{i\omega_n-\varepsilon_{\alpha k}+\mu_0}\boldsymbol{t}_{\alpha k\nu}e^{-i\omega_n\eta}\\ &= \lim_{\eta\to 0^+}\frac{1}{\beta}\sum_n\sum_{\nu'}\mathbf{G}^M_{\mu\nu'}(i\omega_n)\\ &\quad\times\frac{\boldsymbol{\Lambda}_{\alpha\nu'\nu}(x)}{i\omega_n-\Omega x-\bar{\omega}+\mu_0}e^{-i\omega_n\eta}\\ &= -\lim_{\eta,\varepsilon\to 0^+}\frac{1}{\pi}\sum_{\nu'}\int_{-\infty}^{\infty}d\zeta e^{-\zeta\eta}f(\zeta-\mu_0)\\ &\quad\times\Im\left[\frac{\mathbf{G}^r_{\mu\nu'}(\zeta+i\varepsilon)}{\zeta+i\varepsilon-\Omega x-\bar{\omega}}\right]\boldsymbol{\Lambda}_{\alpha\nu'\nu}(x),\end{aligned}\tag{65}$$

in which the last equality comes from the common techniques for summing over all Matsubara frequencies [22] and $f(\zeta)=1/(\exp(\beta\zeta)+1)$.

$$\begin{aligned}\boldsymbol{\psi}_{\alpha'\alpha,\mu\nu}(x',x,t_0) &= \lim_{\eta\to 0^+}\sum_{k\in\alpha}\sum_{k'\in\alpha'}\delta\big(\Omega x+\bar{\omega}-\epsilon_{\alpha k}\big)\\ &\quad\times\delta\big(\Omega x'+\bar{\omega}-\epsilon_{\alpha' k'}\big)t_{\alpha k\nu}t^*_{\alpha' k'\mu}\\ &\quad\times\big[\mathbf{G}^M_{\alpha' k'\alpha k}(0,\eta)-\delta_{\alpha\alpha'}\delta_{kk'}\mathbf{g}^M_{\alpha k}(0,\eta)\big]\\ &= \lim_{\eta\to 0^+}\sum_{k\in\alpha}\sum_{k'\in\alpha'}\sum_{\mu_1\mu_2}\Bigg[t^*_{\alpha' k'\mu}\\ &\quad\times\frac{\delta\big(\Omega x'+\bar{\omega}-\epsilon_{\alpha' k'}\big)}{i\omega_n-\varepsilon_{\alpha' k'}+\mu_0}t_{\alpha' k'\mu_1}\\ &\quad\times\mathbf{G}^M_{\mu_1\mu_2}\big(i\omega_n\big)t^*_{\alpha k\mu_2}\\ &\quad\times\frac{\delta\big(\Omega x+\bar{\omega}-\epsilon_{\alpha k}\big)}{i\omega_n-\varepsilon_{\alpha k}+\mu_0}t_{\alpha k\nu}\Bigg]e^{-i\omega_n\eta}\\ &= -\lim_{\eta,\varepsilon\to 0^+}\frac{1}{\pi}\sum_{\mu_1\mu_2}\boldsymbol{\Lambda}_{\alpha'\mu\mu_1}(x')\\ &\quad\times\int_{-\infty}^{\infty}d\zeta e^{-\zeta\eta}f\big(\zeta-\mu_0\big)\\ &\quad\times\Im\left[\frac{\mathbf{G}^r_{\mu_1\mu_2}\big(\zeta+i\varepsilon\big)}{\big(\zeta+i\varepsilon-\Omega x'-\bar{\omega}\big)\big(\zeta+i\varepsilon-\Omega x-\bar{\omega}\big)}\right]\boldsymbol{\Lambda}_{\alpha\mu_2\nu}(x).\end{aligned}\tag{66}$$

And it is trivial to reproduce the following known result,

$$\boldsymbol{\sigma}(t_0)=-\lim_{\varepsilon\to 0^+}\frac{1}{\pi}\Im\int_{-\infty}^{\infty}d\zeta f(\zeta-\mu_0)\,\mathbf{G}^r(\zeta+i\varepsilon).\tag{67}$$

Using the Kramers-Kronig relationship

$$\boldsymbol{\Sigma}^r_\alpha(z)=-\int_{-1}^{1}dx\frac{\boldsymbol{\Lambda}_\alpha(x)}{x-z},\quad\forall z\in\mathbb{C}\backslash[-1,1]\tag{68}$$

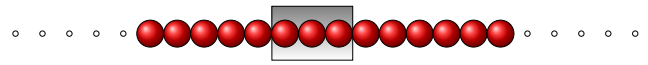

Fig. 1. An illustrative plot showing the 1-D uniform infinite nearest tight-binding chain.

and the identity

$$\frac{T_k(x)-T_k(x')}{x-x'}=U_{k-1}(x')+2\sum_{i=1}^{k-1}U_{k-1-i}(x')T_i(x),\tag{69}$$

where $U_k(x)$ is the Chebyshev polynomial of the second kind, letting $y=(\zeta-\bar{\omega})/\Omega$, we have

see equations (70)–(75) next page.

Now, it is conclusive that neither is this new approach in need of any intractable fitting parameters, nor does it require that the line-width matrix is analytically reproduced as precisely as possible. This is another advantage of this new approach not to be overlooked.

5 Simulation of tight-binding model system

As a preliminary demonstration, it is very instructive to test this new scheme on some simple model system. In this work, the one dimensional (1-D) infinite nearest tight-binding chain is studied, of which, N, neighboring sites in the centre are chosen as the device part and the rest semi-infinite chain on the right/left side as the right/left electrode, respectively. Ordinal number 1 is assigned to leftmost site, and increases from left to right until N. The left boundary between the device part and the electrode is set to be the perpendicular bisector of the segment linking the site 1 in the device part and its left nearest neighbor. The right boundary is similarly defined.

In this model, it is assumed that the local orbitals $|n_j\rangle$'s on each site constitute a complete orthonormal basis set, and the electron is spinless. Since the hopping happens only between nearest neighboring sites, the Hamiltonian for the whole infinite chain is an infinite-dimension tridiagonal real symmetric matrix as follows, with v being the hopping term and μ_0 being the on-site energy, also the Fermi level [23] of the whole infinite chain,

$$\mathbf{H}=\begin{bmatrix}\ddots & \ddots & & & \\ \ddots & \mu_0 & v & & \\ & v & \mu_0 & v & \\ & & v & \mu_0 & \ddots \\ & & & \ddots & \ddots\end{bmatrix}.\tag{76}$$

Due to this special structure, the self-energy $\hat{\boldsymbol{\Sigma}}_\alpha(z)$ is just a scalar function of complex argument z.

In passing, it is pointed out that in this section, a function with the hat symbol on its top, whose argument is not restricted to $[-1,1]$, has not been compounded with the affine map equation (81), and a function which

$$\boldsymbol{\varphi}_{\alpha,0}(t_0) = -\lim_{\varepsilon\to 0^+}\frac{1}{\pi}\Im\int_{-\infty}^{\infty} d\zeta f(\zeta-\mu_0)\,\mathbf{G}^r(\zeta+i\varepsilon)\,\boldsymbol{\Sigma}_\alpha^r(\zeta+i\varepsilon), \tag{70}$$

$$\begin{aligned}\boldsymbol{\varphi}_{\alpha,k\geq 1}(t_0) =& -\lim_{\varepsilon\to 0^+}\frac{2}{\pi}\Im\int_{-\infty}^{\infty} d\zeta f(\zeta-\mu_0)\,\mathbf{G}^r(\zeta+i\varepsilon)\,\boldsymbol{\Sigma}_\alpha^r(\zeta+i\varepsilon)\,T_k(y)\\ &+\lim_{\varepsilon\to 0^+}\frac{2}{\pi}\sum_{l=0}^{k-1}\Im\int_{-\infty}^{\infty} d\zeta f(\zeta-\mu_0)\,\mathbf{G}^r(\zeta+i\varepsilon)\,U_{k-l-1}(y)\boldsymbol{\Lambda}_{\alpha,l},\end{aligned} \tag{71}$$

$$\boldsymbol{\psi}_{\alpha'0,\alpha 0}(t_0) = -\lim_{\varepsilon\to 0^+}\frac{1}{\pi\Omega^2}\Im\int_{-\infty}^{\infty} d\zeta f(\zeta-\mu_0)\,\boldsymbol{\Sigma}_{\alpha'}^r(\zeta+i\varepsilon)\,\mathbf{G}^r(\zeta+i\varepsilon)\,\boldsymbol{\Sigma}_\alpha^r(\zeta+i\varepsilon), \tag{72}$$

$$\begin{aligned}\boldsymbol{\psi}_{\alpha'0,\alpha k\geq 1}(t_0) =& -\lim_{\varepsilon\to 0^+}\frac{2}{\pi\Omega^2}\Im\int_{-\infty}^{\infty} d\zeta f(\zeta-\mu_0)\left[-\boldsymbol{\Sigma}_{\alpha'}^r(\zeta+i\varepsilon)\right]\mathbf{G}^r(\zeta+i\varepsilon)\left[-\boldsymbol{\Sigma}_\alpha^r(\zeta+i\varepsilon)\,T_k(y)+\sum_{l=0}^{k-1}\boldsymbol{\Lambda}_{\alpha,l}U_{k-l-1}(y)\right]\\ =& -\lim_{\varepsilon\to 0^+}\frac{2}{\pi\Omega^2}\Im\int_{-\infty}^{\infty} d\zeta f(\zeta-\mu_0)\,\boldsymbol{\Sigma}_{\alpha'}^r(\zeta+i\varepsilon)\,\mathbf{G}^r(\zeta+i\varepsilon)\,\boldsymbol{\Sigma}_\alpha^r(\zeta+i\varepsilon)\,T_k(y)\\ &+\lim_{\varepsilon\to 0^+}\frac{2}{\pi\Omega^2}\sum_{l=0}^{k-1}\Im\int_{-\infty}^{\infty} d\zeta f(\zeta-\mu_0)\,\boldsymbol{\Sigma}_{\alpha'}^r(\zeta+i\varepsilon)\,\mathbf{G}^r(\zeta+i\varepsilon)\,U_{k-l-1}(y)\boldsymbol{\Lambda}_{\alpha,l},\end{aligned} \tag{73}$$

$$\begin{aligned}\boldsymbol{\psi}_{\alpha'k'\geq 1,\alpha 0}(t_0) =& -\lim_{\varepsilon\to 0^+}\frac{2}{\pi\Omega^2}\Im\int_{-\infty}^{\infty} d\zeta f(\zeta-\mu_0)\left[-\boldsymbol{\Sigma}_{\alpha'}^r(\zeta+i\varepsilon)\,T_{k'}(y)+\sum_{l'=0}^{k'-1}\boldsymbol{\Lambda}_{\alpha',l'}U_{k'-l'-1}(y)\right]\mathbf{G}^r(\zeta+i\varepsilon)\left[-\boldsymbol{\Sigma}_\alpha^r(\zeta+i\varepsilon)\right]\\ =& -\lim_{\varepsilon\to 0^+}\frac{2}{\pi\Omega^2}\Im\int_{-\infty}^{\infty} d\zeta f(\zeta-\mu_0)\,\boldsymbol{\Sigma}_{\alpha'}^r(\zeta+i\varepsilon)\,\mathbf{G}^r(\zeta+i\varepsilon)\,\boldsymbol{\Sigma}_\alpha^r(\zeta+i\varepsilon)\,T_{k'}(y)\\ &+\lim_{\varepsilon\to 0^+}\frac{2}{\pi\Omega^2}\sum_{l'=0}^{k'-1}\boldsymbol{\Lambda}_{\alpha',l'}\Im\int_{-\infty}^{\infty} d\zeta f(\zeta-\mu_0)\,\mathbf{G}^r(\zeta+i\varepsilon)\,\boldsymbol{\Sigma}_\alpha^r(\zeta+i\varepsilon)\,U_{k'-l'-1}(y),\end{aligned} \tag{74}$$

$$\begin{aligned}\boldsymbol{\psi}_{\alpha'k'\geq 1,\alpha k\geq 1}(t_0) =& -\lim_{\varepsilon\to 0^+}\frac{4}{\pi\Omega^2}\Im\int_{-\infty}^{\infty} d\zeta f(\zeta-\mu_0)\left[-\boldsymbol{\Sigma}_{\alpha'}^r(\zeta+i\varepsilon)\,T_{k'}(y)+\sum_{l'=0}^{k'-1}\boldsymbol{\Lambda}_{\alpha',l'}U_{k'-l'-1}(y)\right]\mathbf{G}^r(\zeta+i\varepsilon)\\ &\times\left[-\boldsymbol{\Sigma}_\alpha^r(\zeta+i\varepsilon)\,T_k(y)+\sum_{l=0}^{k-1}\boldsymbol{\Lambda}_{\alpha,l}U_{k-l-1}(y)\right]\\ =& -\lim_{\varepsilon\to 0^+}\frac{4}{\pi\Omega^2}\Im\int_{-\infty}^{\infty} d\zeta f(\zeta-\mu_0)\,\boldsymbol{\Sigma}_{\alpha'}^r(\zeta+i\varepsilon)\,\mathbf{G}^r(\zeta+i\varepsilon)\,\boldsymbol{\Sigma}_\alpha^r(\zeta+i\varepsilon)\,T_{k'}(y)T_k(y)\\ &+\lim_{\varepsilon\to 0^+}\frac{4}{\pi\Omega^2}\sum_{l=0}^{k-1}\Im\int_{-\infty}^{\infty} d\zeta f(\zeta-\mu_0)\,\boldsymbol{\Sigma}_{\alpha'}^r(\zeta+i\varepsilon)\,\mathbf{G}^r(\zeta+i\varepsilon)\,T_{k'}(y)U_{k-l-1}(y)\boldsymbol{\Lambda}_{\alpha,l}\\ &+\lim_{\varepsilon\to 0^+}\frac{4}{\pi\Omega^2}\sum_{l'=0}^{k'-1}\boldsymbol{\Lambda}_{\alpha',l'}\Im\int_{-\infty}^{\infty} d\zeta f(\zeta-\mu_0)\,\mathbf{G}^r(\zeta+i\varepsilon)\,\boldsymbol{\Sigma}_\alpha^r(\zeta+i\varepsilon)\,U_{k'-l'-1}(y)T_k(y)\\ &-\lim_{\varepsilon\to 0^+}\frac{4}{\pi\Omega^2}\sum_{l'=0}^{k'-1}\sum_{l=0}^{k-1}\boldsymbol{\Lambda}_{\alpha',l'}\Im\int_{-\infty}^{\infty} d\zeta f(\zeta-\mu_0)\,\mathbf{G}^r(\zeta+i\varepsilon)\,U_{k'-l'-1}(y)U_{k-l-1}(y)\boldsymbol{\Lambda}_{\alpha,l}.\end{aligned} \tag{75}$$

is not matrix-valued is not represented in bold symbol. Specifically, the effective Hamiltonian of the device part is a $N\times N$ tridiagonal matrix, not Hermitian but complex symmetric,

$$\boldsymbol{h}+\hat{\boldsymbol{\Sigma}}(z) = \begin{bmatrix}\mu_0+\hat{\Sigma}_L(z) & v & & & \\ v & \ddots & \ddots & & \\ & \ddots & \ddots & v & \\ & & v & \mu_0+\hat{\Sigma}_R(z)\end{bmatrix}_{N\times N}. \tag{77}$$

Being a scalar function, $\hat{\Sigma}_\alpha(z)$ can be analytically calculated owing to the recursion relationship [24]

$$\hat{\Sigma}_\alpha(z) = v^2\left[z-\mu_0-\hat{\Sigma}_\alpha(z)\right]^{-1}. \tag{78}$$

This equation has solution

$$\hat{\Sigma}_\alpha(z) = \frac{z-\mu_0}{2}-|v|\left[\left(\frac{z-\mu_0}{2|v|}\right)^2-1\right]^{\frac{1}{2}}. \tag{79}$$

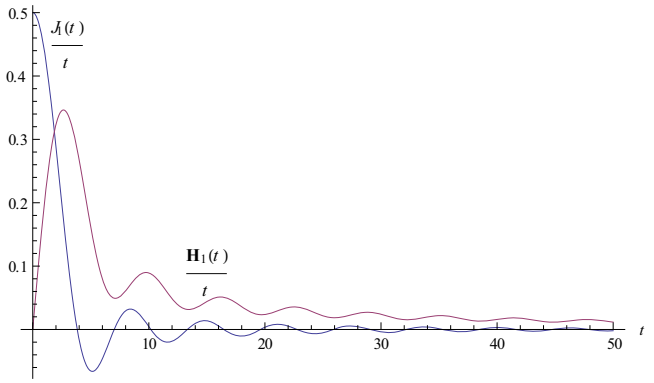

Fig. 2. Real and imaginary part of equilibrium lesser self-energy $\boldsymbol{\Sigma}_\alpha^<(t)$ for $v = 1$, $\Omega = 1$.

The choice of branch of this multi-valued function $\left(z^2-1\right)^{\frac{1}{2}}$ is such that on the top edge of its branch cut it has a positive imaginary part, i.e.

$$\hat{\Sigma}_\alpha^r(\omega) = \left(\frac{\omega-\mu_0}{2}\right) - i|v|\sqrt{1-\left(\frac{\omega-\mu_0}{2|v|}\right)^2} \tag{80}$$

where the argument $\omega \in [\mu_0 - 2|v|, \mu_0 + 2|v|]$.

It is ready to see that the two constants $\bar{\omega}$ and Ω of this model system are just μ_0 and $2|v|$, respectively.

In terms of the new argument,

$$x = \frac{\omega-\mu_0}{2|v|}, \quad x \in [-1, 1], \tag{81}$$

we have

$$\Sigma_\alpha^r(x) = |v|\left(x - i\sqrt{1-x^2}\right), \tag{82}$$

$$\Lambda_\alpha(x) = \frac{|v|}{\pi}\sqrt{1-x^2}. \tag{83}$$

Here, since the analytic expression of $\Lambda_\alpha(x)$ is known, the equilibrium lesser self-energy $\boldsymbol{\Sigma}_\alpha^<(\tau,t)$ can be explicitly expressed by some known special functions at zero temperature,

$$\begin{aligned}\boldsymbol{\Sigma}_\alpha^<(\tau,t) &= i\int_{-1}^{0} dx \frac{|v|}{\pi}\sqrt{1-x^2}e^{i\Omega x(t-\tau)} \\ &= \frac{|v|H_1(\Omega(t-\tau))}{\Omega(t-\tau)} + i\frac{|v|J_1(\Omega(t-\tau))}{\Omega(t-\tau)},\end{aligned} \tag{84}$$

in which H_n is the Struve function of the integer-order, whose definition can be found in reference [18].

In particular, according to the asymptotic expansions of Bessel function and Struve function [18], it is emphasized that $\boldsymbol{\Sigma}_\alpha^<(\tau,t)$ for this specific model, which is plotted in Figure 2, does NOT decay exponentially but only *algebraically* as $(t-\tau) \to \infty$.

In this model system, the $\boldsymbol{\Lambda}_{\alpha,k}(x)$'s, the definition of which is in equation (37), are also actually scalars and simple,

$$\Lambda_\alpha(x)\pi\sqrt{1-x^2} = |v|\left(1-x^2\right) = \frac{|v|}{2}T_0(x) - \frac{|v|}{2}T_2(x), \tag{85}$$

which means, only $\Lambda_{\alpha,0} = |v|/2$ and $\Lambda_{\alpha,2} = -|v|/2$, are non-zero, rendering the computation of $\boldsymbol{\Pi}_{\alpha,k}(t)$ very easy.

$$\begin{aligned}\boldsymbol{\Xi}_{\alpha,0}(t_0) &= \int_{-1}^{1} dx\, \bar{f}_\alpha(x)\boldsymbol{\Lambda}_\alpha(x) \\ &= -\frac{|v|}{2\pi}\int_{-1}^{1} dx \frac{\bar{f}(x)(1-T_2(x))}{\sqrt{1-x^2}},\end{aligned} \tag{86}$$

$$\begin{aligned}\boldsymbol{\Xi}_{\alpha,1}(t_0) &= \int_{-1}^{1} dx\, T_1(x)\bar{f}_\alpha(x)\boldsymbol{\Lambda}_\alpha(x) \\ &= \frac{|v|}{4\pi}\int_{-1}^{1} dx \frac{\bar{f}(x)(T_1(x)-T_3(x))}{\sqrt{1-x^2}},\end{aligned} \tag{87}$$

$$\begin{aligned}\boldsymbol{\Xi}_{\alpha,k}(t_0) &= \int_{-1}^{1} dx\, T_k(x)\bar{f}_\alpha(x)\boldsymbol{\Lambda}_\alpha(x) \\ &= \frac{|v|}{2\pi}\int_{-1}^{1} dx \frac{\bar{f}(x)T_k(x)}{\sqrt{1-x^2}} \\ &\quad - \frac{|v|}{4\pi}\int_{-1}^{1} dx \frac{\bar{f}(x)T_{k+2}(x)}{\sqrt{1-x^2}} \\ &\quad - \frac{|v|}{4\pi}\int_{-1}^{1} dx \frac{\bar{f}(x)T_{k-2}(x)}{\sqrt{1-x^2}}.\end{aligned} \tag{88}$$

As is known in reference [25], the retarded Green's function of the device part is

$$\begin{aligned}\langle n_2|\mathbf{G}^r(x)|n_1\rangle &= \frac{-i\left(x - i\sqrt{1-x^2}\right)^{|n_2-n_1|}}{2|v|\sqrt{1-x^2}} \\ &= \frac{-i\,e^{-i|n_2-n_1|\arccos x}}{2|v|\sqrt{1-x^2}}.\end{aligned} \tag{89}$$

To make an explicit connection between this formulation and matrix representation, we decompose a $N \times N$ constant matrix full of 1 into a series of real symmetric matrices $\{\mathbf{G}_k\}_0^{N-1}$, with its entries defined by the following

$$\langle m|\mathbf{G}_k|n\rangle = \begin{cases} 1 \text{ if } |m-n| = k \\ 0 \text{ otherwise.}\end{cases} \tag{90}$$

Therefore, we have the following decomposition:

$$\mathbf{G}^r(x) = \frac{-i\sum_{k=0}^{N-1}\mathbf{G}_k e^{-ik\arccos x}}{2|v|\sqrt{1-x^2}}. \tag{91}$$

With the help of this formulation, we can go on to determine the initial condition for HEOM,

$$\begin{aligned}\boldsymbol{\sigma}(t_0) &= -\frac{\Omega}{\pi}\Im\int_{-1}^{1} dx \bar{f}(x)\mathbf{G}^r(x) \\ &= \sum_{k=0}^{N}\frac{\Omega\mathbf{G}_k}{2\pi|v|}\Re\int_{-1}^{1} dx \frac{\bar{f}(x)e^{-ik\arccos x}}{\sqrt{1-x^2}} \\ &= \sum_{k=0}^{N}\frac{\Omega\mathbf{G}_k}{2\pi|v|}\int_{-1}^{1} dx \frac{\bar{f}(x)T_k(x)}{\sqrt{1-x^2}}.\end{aligned} \tag{92}$$

The formulas for $\boldsymbol{\varphi}_{\alpha,k}(t_0)$'s and $\boldsymbol{\psi}_{\alpha'k',\alpha k}(t_0)$'s can be found in Appendix.

Notice that in this model system $\mu_0 = \bar{\omega}$, hence, $\bar{f}(x) = \left(1 + e^{\beta\Omega x}\right)^{-1}$.

From this, it can be shown that the terms in equation (92) with $k = 2n, n \in \mathbb{N}$, vanish identically and

$$\int_{-1}^{1} \frac{\bar{f}(x)dx}{\sqrt{1-x^2}} = \frac{1}{2}. \tag{93}$$

Particularly, at zero temperature, all these integrals can be calculated by hand. However, at finite temperature, especially at lower temperature, these integrals are not so easy to handle and we resort to some advanced techniques [26,27].

With the initial condition ready, we can go on to advance equations (39), (40) and (41). In this work, all the bias voltages are of the form $\Delta_L(t) = -\Delta_R(t)$, i.e. symmetrically applied to left electrode and right electrode, respectively. And since the Hartree potential does not show up in the tight-binding description, there is no need calculating the new Hartree potential as a response to variation of the charge density of the device part by solving the Poisson equation. Rather, the voltage drop across the device part can be reasonably assumed to be linear with the abscissa. Specifically, in the transient regime, the Hamiltonian of the device part takes into account the voltage drop by simply altering the on-site energy of each site. Take kth site for example, the dynamic change of its on-site energy is calculated as follows,

$$\delta\boldsymbol{h}_{kk}(t) = (k - 0.5)(\Delta_R(t) - \Delta_L(t))/N + \Delta_L(t), \tag{94}$$

where 0.5 reflects that the voltage drop starts exactly with the left boundary and ends exactly at the right boundary. This assumption is compatible with the so-called gauge-invariance requirement [28]. Actually, equations (39), (40) and (41) are left invariant when bias voltage is simultaneously shifted by a constant. This can be easily verified. Bias voltage does not present in equation (39), and the difference between $\Delta_{\alpha'}(t)$ and $\Delta_\alpha(t)$ in equation (41) is not affected by such a simultaneous shift, and the time-dependent part of

$$\boldsymbol{h}(t) - \Delta_L(t) = \boldsymbol{h}(t_0) + \delta\boldsymbol{h}(t) - \Delta_L(t)$$

in equation (40) is proportional to $(\Delta_R(t) - \Delta_L(t))$, so is $(\boldsymbol{h}(t) - \Delta_R(t))$. Thus the current should be invariant under such a simultaneous shift of bias voltage.

Without loss of non-commutativity of matrix algebra yet not causing too much complexity, we take $N = 3$ for instance. In this case, the matrices needed in the decomposition of retarded Green's function is given below by the definition equation (90),

$$\mathbf{G}_0 = \begin{bmatrix} 1 & 0 & 0 \\ 0 & 1 & 0 \\ 0 & 0 & 1 \end{bmatrix}, \mathbf{G}_1 = \begin{bmatrix} 0 & 1 & 0 \\ 1 & 0 & 1 \\ 0 & 1 & 0 \end{bmatrix}, \mathbf{G}_2 = \begin{bmatrix} 0 & 0 & 1 \\ 0 & 0 & 0 \\ 1 & 0 & 0 \end{bmatrix}. \tag{95}$$

And in our simulation we assume $v = 1.0$, $\mu_0 = 1.5$. The desired length of propagation time is $t_{max} = 15$. The bias voltage is of the form $\Delta_L = 0.05\vartheta(t - t_0)$, a step-like function. As top priority, the total number k_{max} of modified moments $\boldsymbol{\varphi}_{\alpha,k}(t)$'s needed in the simulation interval $[0, 15]$ should be determined, based on which the total number of modified moments $\boldsymbol{\psi}_{\alpha'k',\alpha k}(t)$'s can also be known. As mentioned in Section 3, the spectrally decaying factor $J_n(\Omega t_{max})$ plays the key role in truncating the infinite series in equations (39) and (40) at $t = t_{max}$. Here, the unique k_{max} is found by the following inequalities:

$$J_{k_{max}}(\Omega(t - t_0)) \geq 10^{-12},\ J_{k_{max}+1}(\Omega(t - t_0)) < 10^{-12}. \tag{96}$$

The Bessel function of the first kind of integer order can be calculated to the machine precision by the subroutine '`bessel_jn`' internalized in the Fortran 2008 standard. Then the initial conditions are calculated according to equations (92), (A.1), (A.2), (A.3), (A.4), (A.5), (A.6), (A.7), (A.8) and (A.9). After this, the bias voltage is turned on and the explicit fourth-order Runge-Kutta (RK4) algorithm is employed to advance equations (39), (40) and (41), with the time step being 0.03. In this process, at a given time t, a train of $J_{0\leq k\leq k_0}(\Omega(t - t_0))$'s which are not less than 10^{-12}, complying with the same criterion of truncation in equation (96), are calculated so that only $\boldsymbol{\varphi}_{\alpha,0\leq k\leq k_0}(t)$'s have sensible contributions to the dissipation functional and the transient current. With these non-negligible $J_k(\Omega(t - t_0))$'s, $\Pi_{\alpha,k}(t)$'s, $\Xi_{\alpha,k}(t)$'s are computed according to equations (36) and (38) on the fly.

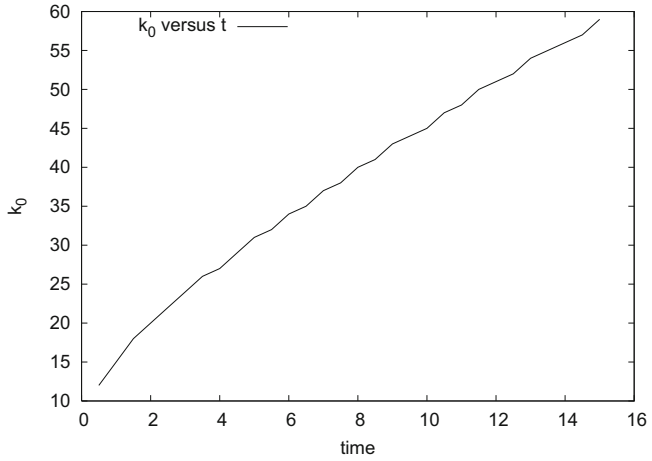

Fig. 3. k_0 against time such that $J_{0\leq k\leq k_0}(\Omega(t - t_0)) \geq 10^{-12}$.

To make it palpable, some k_0's corresponding to different time t are plotted in Figure 3 for this specific choice of parameter in this model system, through which it is confirmed that k_0 scales linearly with t.

Simulation results at zero temperature are reported in this subsection. The transient current depicted in Figure 4a says that the left current and right current in both cases are exactly opposite to each other in the simulation time and supposedly in later times, while the current depicted in Figure 4b corresponds to those with two different time increments, 0.05 and 0.005, respectively.

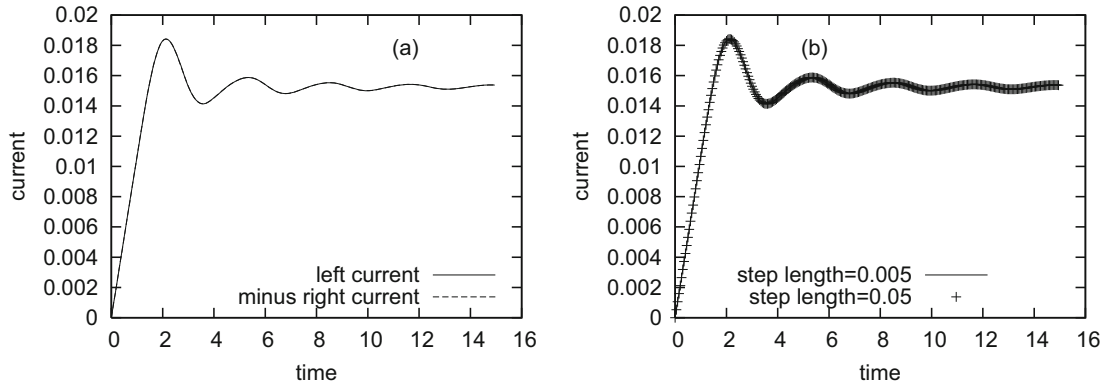

Fig. 4. (a) The left current and the minus right current of 3 sites as the device part under the symmetric bias voltage $\Delta_L = 0.05\vartheta(t - t_0)$; (b) the left currents with two different lengths of time step.

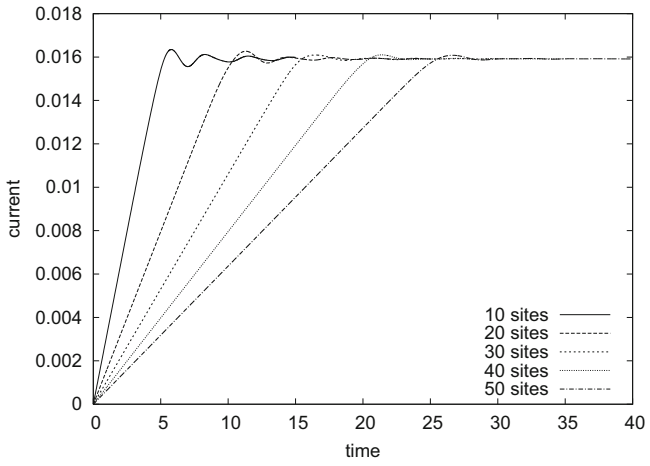

Fig. 5. The left current of multi-sites under bias voltage $\Delta_L(t) = 0.05\vartheta(t - t_0)$.

The most interesting finding in this model system is that the transient current of the system with more than 10 sites in the device part increases linearly with time in the initial stage [29], as shown in Figure 5.

Some more simulation results related to the effect of temperature and length of the device in this model system can be found in references [7,30].

6 Conclusions and discussions

In this paper, a more general framework which respects the non-uniformity of the conduction band profile and finiteness of the bandwidths is proposed to tackle the time-dependent quantum transport at zero as well as finite temperature. This new approach enjoys several merits, especially it does not rely on any parametrization, hence it can be directly integrated with the first-principles simulations. As indicated in Section 5, the time complexity of this approach is $O(N^3)$, where N is the number of steps from t_0 to the maximum simulation time t_{max}, since the total numbers of modified moments $\boldsymbol{\varphi}_{\alpha,k}(t)$'s and $\boldsymbol{\psi}_{\alpha'k',\alpha k}(t)$'s needed are $O(N)$ and $O(N^2)$, respectively. The possibility to reduce the time complexity of the present approach while still retaining the accuracy is being under consideration.

Up to now, this method has been tested on model systems only, and already given rise to a series of exciting results. To our knowledge, application of HEOM to dynamics at zero temperature is reported for the first time.

We add some remarks to conclude this work. Penetrative audience may notice that $\Lambda_\alpha(x)$ in equation (83) is nothing but the weight function of Chebyshev polynomial of the second kind except for the constant coefficient. Although this is never a curious coincidence, such a godsend will not happen under non-orthogonal basis set when we deal with realistic simulation, unfortunately.

The audience may also notice that in this work the compactness of the support of the line-width matrix $\boldsymbol{\Lambda}(\omega)$ is taken for granted but not been justified a priori and how to determine the important parameters ω_{min} and ω_{max} has not been explained. Actually, these issues have some connection with spectral property of special operators, which will be looked into in future publication.

Support from the Hong Kong Research Grant Council (Contracts Nos. HKU700909P, 700912P, 700711P and HKUST 9/CRF/11G), and the University Grant Council (Contract No. AoE/P-04-08) is gratefully acknowledged.

Appendix: Initial condition for the model system in Section 5

With the general integral representation of $\boldsymbol{\varphi}_{\alpha,k}(t_0)$'s and $\boldsymbol{\psi}_{\alpha'k',\alpha k}(t_0)$'s, it is found that $\boldsymbol{\varphi}_{\alpha,k}(t_0)$'s are just $N \times 1$ matrices, or simply vectors occupying either the first or the last column of a $N \times N$ matrix, and $\boldsymbol{\psi}_{\alpha'k',\alpha k}(t_0)$'s are just 1×1 matrices, or simply scalars occupying one of the four corners of a $N \times N$ matrix. So are the corresponding time-dependent ones.

$$\begin{aligned}\boldsymbol{\varphi}_{\alpha,0}(t_0) &= -\frac{1}{\pi}\Im\int_{-1}^{1} dx \bar{f}(x)\mathbf{G}^r(x)\,\boldsymbol{\Sigma}^r_\alpha(x) \\ &= \sum_{k=0}^{N-1}\frac{\mathbf{G}_k|n_\alpha\rangle}{2\pi}\int_{-1}^{1} dx\frac{\bar{f}(x)T_{k+1}(x)}{\sqrt{1-x^2}} \qquad \text{(A.1)}\end{aligned}$$

$$\begin{aligned}\boldsymbol{\varphi}_{\alpha,1}(t_0) &= \frac{2}{\pi\Omega}\Im\left[\int_{-\infty}^{\infty} d\zeta f\left(\zeta-\mu_0\right)\hat{\mathbf{G}}^r\left(\zeta\right)\right.\\ &\left.\times\int_{-1}^{1} dx\frac{\boldsymbol{\Lambda}_\alpha(x)T_1(x)}{x-\frac{\zeta-\bar{\omega}}{\Omega}-i\varepsilon}\right]\\ &= \frac{1}{\pi\Omega}\Im\left[\int_{-\infty}^{\infty} d\zeta f\left(\zeta-\mu_0\right)\hat{\mathbf{G}}^r\left(\zeta\right)\right.\\ &\left.\times\int_{-1}^{1} dx\frac{\boldsymbol{\Lambda}_\alpha(x)U_1(x)}{x-\frac{\zeta-\bar{\omega}}{\Omega}-i\varepsilon}\right]\\ &= \sum_{k=0}^{N-1}\frac{\mathbf{G}_k|n_\alpha\rangle}{2\pi}\int_{-1}^{1} dx\frac{\bar{f}(x)T_{k+2}(x)}{\sqrt{1-x^2}}\end{aligned} \tag{A.2}$$

$$\begin{aligned}\boldsymbol{\varphi}_{\alpha,l\geq 2}(t_0) &= \frac{2}{\pi\Omega}\Im\left[\int_{-\infty}^{\infty} d\zeta f\left(\zeta-\mu_0\right)\hat{\mathbf{G}}^r\left(\zeta\right)\right.\\ &\left.\times\int_{-1}^{1} dx\frac{\boldsymbol{\Lambda}_\alpha(x)T_l(x)}{x-\frac{\zeta-\bar{\omega}}{\Omega}-i\varepsilon}\right]\\ &= \frac{1}{\pi\Omega}\Im\left[\int_{-\infty}^{\infty} d\zeta f\left(\zeta-\mu_0\right)\hat{\mathbf{G}}^r\left(\zeta\right)\right.\\ &\left.\times\int_{-1}^{1} dx\frac{\boldsymbol{\Lambda}_\alpha(x)U_l(x)-\boldsymbol{\Lambda}_\alpha(x)U_{l-2}(x)}{x-\frac{\zeta-\bar{\omega}}{\Omega}-i\varepsilon}\right]\\ &= \sum_{k=0}^{N-1}\frac{\mathbf{G}_k|n_\alpha\rangle}{2\pi}\int_{-1}^{1} dx\frac{\bar{f}(x)\left(T_{k+l+1}(x)-T_{k+l-1}(x)\right)}{\sqrt{1-x^2}}\end{aligned} \tag{A.3}$$

$$\begin{aligned}\psi_{\alpha'0,\alpha0}(t_0) &= -\frac{1}{\pi\Omega}\Im\int_{-1}^{1} dx\boldsymbol{\Sigma}^r_{\alpha'}(x)\bar{f}(x)\mathbf{G}^r(x)\boldsymbol{\Sigma}^r_{\alpha}(x)\\ &= \sum_{k=0}^{N-1}\frac{|v|\langle n_{\alpha'}|\mathbf{G}_k|n_\alpha\rangle}{2\pi\Omega}\int_{-1}^{1} dx\frac{\bar{f}(x)T_{k+2}(x)}{\sqrt{1-x^2}}\end{aligned} \tag{A.4}$$

$$\begin{aligned}\psi_{\alpha'0,\alpha1}(t_0) &= 2\int_{-1}^{1} dx'\int_{-1}^{1} dx\boldsymbol{\psi}_{\alpha',\alpha}(x',x,t_0)T_1(x)\\ &= \sum_{k=0}^{N-1}\frac{|v|\langle n_{\alpha'}|\mathbf{G}_k|n_\alpha\rangle}{2\pi\Omega}\int_{-1}^{1} dx\frac{\bar{f}(x)T_{k+3}(x)}{\sqrt{1-x^2}}\end{aligned} \tag{A.5}$$

$$\begin{aligned}\psi_{\alpha'0,\alpha l\geq 2}(t_0) &= 2\int_{-1}^{1} dx'\int_{-1}^{1} dx\boldsymbol{\psi}_{\alpha',\alpha}(x',x,t_0)T_l(x)\\ &= \sum_{k=0}^{N-1}\frac{|v|\langle n_{\alpha'}|\mathbf{G}_k|n_\alpha\rangle}{2\pi\Omega}\\ &\times\int_{-1}^{1} dx\frac{\bar{f}(x)\left(T_{k+l+2}(x)-T_{k+l}(x)\right)}{\sqrt{1-x^2}}\end{aligned} \tag{A.6}$$

$$\begin{aligned}\psi_{\alpha'1,\alpha1}(t_0) &= 4\int_{-1}^{1} dx'\int_{-1}^{1} dx\boldsymbol{\psi}_{\alpha',\alpha}(x',x,t_0)T_1(x')T_1(x)\\ &= \sum_{k=0}^{N-1}\frac{|v|\langle n_{\alpha'}|\mathbf{G}_k|n_\alpha\rangle}{2\pi\Omega}\int_{-1}^{1} dx\frac{\bar{f}(x)T_{k+4}(x)}{\sqrt{1-x^2}}\end{aligned} \tag{A.7}$$

$$\begin{aligned}\psi_{\alpha'1,\alpha l\geq 2}(t_0) &= 4\int_{-1}^{1} dx'\int_{-1}^{1} dx\boldsymbol{\psi}_{\alpha',\alpha}(x',x,t_0)T_1(x')T_l(x)\\ &= \sum_{k=0}^{N-1}\frac{|v|\langle n_{\alpha'}|\mathbf{G}_k|n_\alpha\rangle}{2\pi\Omega}\\ &\times\int_{-1}^{1} dx\frac{\bar{f}(x)\left(T_{k+l+3}(x)-T_{k+l+1}(x)\right)}{\sqrt{1-x^2}}\end{aligned} \tag{A.8}$$

$$\psi_{\alpha' l'\geq 2,\alpha l\geq 2}(t_0) = 4\int_{-1}^{1} dx'\int_{-1}^{1} dx\boldsymbol{\psi}_{\alpha',\alpha}(x',x,t_0)$$

$$\begin{aligned}T_{l'}(x')T_l(x) &= \sum_{k=0}^{N-1}\frac{|v|\langle n_{\alpha'}|\mathbf{G}_k|n_\alpha\rangle}{2\pi\Omega}\\ &\times\int_{-1}^{1} dx\bar{f}(x)\frac{T_{k+l'+l+2}(x)-2T_{k+l'+l}(x)+T_{k+l'+l-2}(x)}{\sqrt{1-x^2}}.\end{aligned} \tag{A.9}$$

Here, $|n_\alpha\rangle$ means the unit vector corresponding to the first or last column of a $N\times N$ matrix.

References

1. J. Taylor, H. Guo, J. Wang, Phys. Rev. B **63**, 245407 (2001)
2. M. Brandbyge, J.-L. Mozos, P. Ordejón, J. Taylor, K. Stokbro, Phys. Rev. B **65**, 165401 (2002)
3. Y.Q. Xue, S. Datta, M.A. Ratner, Chem. Phys. **281**, 151 (2002)
4. X. Zheng, F. Wang, C.Y. Yam, Y. Mo, G.H. Chen, Phys. Rev. B **75**, 195127 (2007)
5. E. Runge, E.K.U. Gross, Phys. Rev. Lett. **52**, 997 (1984)
6. X. Zheng, G.H. Chen, Y. Mo, S.K. Koo, H. Tian, C.Y. Yam, Y.J. Yan, J. Chem. Phys. **133**, 114101 (2010)
7. H. Tian, Ph.D. thesis, University of Hong Kong, 2012
8. J.S. Jin, X. Zheng, Y.J. Yan, J. Chem. Phys. **128**, 234703 (2008)
9. A. Croy, U. Saalmann, Phys. Rev. B **80**, 245311 (2009)
10. T. Ozaki, Phys. Rev. B **75**, 035123 (2007)
11. J. Hu, R.X. Xu, Y.J. Yan, J. Chem. Phys. **133**, 101106 (2010)
12. A.-P. Jauho, N.S. Wingreen, Y. Meir, Phys. Rev. B **50**, 5528 (1994)
13. M. Cini, Phys. Rev. B **22**, 5887 (1980)
14. A. Iserles, IMA J. Numer. Anal. **24**, 365 (2004)
15. N.S. Bakhvalov, L.G. Vasileva, USSR Comput. Math. Math. Phys. **8**, 241 (1968)

16. T.N.L. Patterson, Numer. Math. **27**, 41 (1976)
17. J.C. Mason, D.C. Handscomb, *Chebyshev Polynomials* (Chapman & Hall/CRC, 2003)
18. M. Abramowitz, I.A. Stegun, *Handbook of Mathematical Functions* (Dover, New York, 1965)
19. A.L. Fetter, J.D. Walecka, *Quantum Theory of Many-particle Systems* (Dover, New York, 2003)
20. R. Kubo, J. Phys. Soc. Jpn **12**, 570 (1957)
21. P.C. Martin, J. Schwinger, Phys. Rev. **115**, 1342 (1959)
22. H. Bruus, K. Flensberg, *Many-body Quantum Theory in Condensed Matter Physics: an introduction* (Oxford University Press, 2004)
23. C. Kittel, *Introduction to Solid State Physics* (Wiley, New Jersey, 2005)
24. I. Appelbaum, T. Wang, J.D. Joannopoulos, V. Narayanamurti, Phys. Rev. B **69**, 165301 (2004)
25. E.N. Economou, *Green's Functions in Quantum Physics* (Springer-Verlag, New York, 2006)
26. W. Gautschi, Numer. Algorithms **63**, 369 (2013)
27. H. Tian, unpublished
28. M. Büttiker, J. Phys.: Condens. Matter **5**, 9361 (1993)
29. S.G. Chen, H. Xie, Y. Zhang, X.D. Cui, G.H. Chen, Nanoscale **5**, 169 (2013)
30. H. Tian, G.H. Chen, J. Chem. Phys. **137**, 204114 (2012)